

**HYDRAULIC SPRAYER CONTROL FOR THE  
QUENCHING OF Mg ALLOYS**

**HYDRAULIC SPRAYER CONTROL FOR THE  
COOLING AND QUENCHING OF MAGNESIUM  
AND ALUMINIUM ALLOYS**

By HINO K PRINGNITZ, B.ENG

A Thesis Submitted to the School of Graduate Studies in  
Partial Fulfillment of the Requirements for the Degree: Master  
of Applied Science in Engineering

McMaster University

© Copyright by H.K.H Pringnitz September 2015

McMaster University MASTER OF APPLIED SCIENCE IN  
ENGINEERING (2015) Hamilton, Ontario (Mechanical Engineering)

**TITLE:** HYDRAULIC SPRAYER CONTROL FOR THE COOLING  
AND QUENCHING OF MAGNESIUM AND ALUMINIUM ALLOYS

**AUTHOR:** Hino K. H. Pringnitz, B.Eng. (McMaster University)

**CO-SUPERVISOR:** Dr. Gary Bone

**CO-SUPERVISOR:** Dr. Sumanth Shankar

**NUMBER OF PAGES:** no, xvii, 108

**LAY ABSTRACT**

During the sand casting of aluminium and magnesium rapid cooling will greatly improve the material properties. By containing the liquid metal in a water soluble sand mould, and spraying it with water; the desired part shape and rapid cooling can be achieved. Removing the mould requires a powerful high flow rate jet. During the solidification of the metal, the flow rate must be reduced or the part would be demolished. This necessitated the development of a high speed, high flow rate controller to adjust the flow rate to remove the sand but not damage the part, and to maintain a smooth continuous cooling rate. The hydraulic system being controlled consists of three electronic valves connected to six spray nozzles. Several controllers are developed and compared experimentally. The best controller is shown to provide a quick and precise response.

**ABSTRACT**

For over 30 years research has been done concerning the solidification and quenching of light metal alloys for the purpose of improving material properties. This thesis is concerned with an interesting new process for casting metals, by spraying water onto a sand mould, removing the sand and the directly quenching the part. This process is challenging since the component during solidification is extremely fragile, and the rate of cooling that is needed could seriously damage it. The water flow rate to the component needs to be quickly and precisely controlled. Additionally as this a new method there is very little prior art.

The purpose of this thesis to develop a control system for the water sprayers flow rates. With this system the flow rate through the nozzles will be controlled indirectly using pressure feedback. The material properties and casting process, and how they influenced the design and construction of the spraying apparatus, are explained first. The hydraulic plant being controlled consists of three proportional valves connected to six spray nozzles. Based on experiments, the plant is extremely nonlinear making it difficult to control.

Several controllers were developed and compared experimentally. The best performance was produced by extending a proportional plus integral plus derivative controller by adding an empirical nonlinear feedforward component; smoothing the setpoint; bounding the integration term; adding one bias at time zero and a 2<sup>nd</sup> bias for the remaining time (to mitigate valve stiction and to prime the hoses). This extended PID controller produced a 0.7% mean error and 1.9% mean absolute error for a

multi-step setpoint covering a range of 0 to 80 PSI. Its performance was also highly repeatable. The standard deviations of the mean error, mean absolute error and maximum absolute error were less than 0.2 PSI over five runs.

## ACKNOWLEDGMENTS

- I would like to acknowledge the industrial partners whom supported this project
- Canmet Materials for the technical support received.
- Thanks to Dr. Sumanth Shankar for giving me this chance
- Dr. Gary Bone for guiding, editing and controls knowledge.
- The members of my defense committee, Dr. Fengjun Yan and Dr. Mohamed Hamed for taking their time to review my thesis.
- Special thanks to Dr. Kifah Takrouri, Aykut Dursun, Carolyn Holdings, and Jessie for their help and suggestions in conducting the experiments.
- The entire Mechanical Engineering Machine Shop
- Nicholas Andrea for starting my in a strange path
- Finally thanks my friends for being there when I needed them most.

**TABLE OF CONTENTS**

Lay Abstract .....	iii
Abstract.....	iv
Acknowledgments.....	vi
Table of Contents .....	vii
Tables .....	xii
Figure.....	xiii
Abbreviations.....	xvi
Nomenclature .....	xvii
Chapter 1. INTRODUCTION1.....	
1.1 New Casting Technology .....	3
1.2 Organization of this Thesis .....	7
Chapter 2. Literature Review .....	8
2.1 Introduction.....	8
2.2 Spray Cooling of Materials.....	9
2.3 Control of Agricultural Sprayers.....	11
2.4 Control of Water Hydraulic and Pneumatic Actuators .....	12
2.5 Bottom cooling and Coolant Accumulation .....	15
2.6 Solidification Front and Casting Flaw Behavior .....	15
2.7 Fellow researcher Aykut Dursun .....	19
2.8 Summary.....	20

Chapter 3. Apparatus Design.....	22
3.1 Introduction.....	22
3.2 Justification of a Stationary Sequential Sprayer Setup.....	22
3.3 Containment Chamber .....	24
3.4 Valve Selection .....	25
3.4.1 Pulse Width Modulation Valves.....	25
3.4.2 Proportional Solenoid.....	26
3.5 Pressure sensors .....	27
3.6 System Design and Peripherals .....	28
3.7 Summary.....	29
Chapter 4. Plant behavior.....	<b>Error! Bookmark not defined.</b>
4.1 Introduction.....	30
4.2 Plant Overview.....	30
4.3 Challenging dynamic behaviors.....	31
4.3.1 Pressure noise.....	31
4.3.2 Valve stiction.....	32
4.3.3 Water hammer.....	33
4.3.4 Plant nonlinearity and its mitigation.....	34
4.4 Conclusion .....	40
Chapter 5. Controller Development.....	41
5.1 Introduction.....	41
5.2 PID Controller .....	42
5.2.1 Introduction.....	42

5.2.2	PID Results .....	44
5.3	Development of PID plus feedforward controller .....	49
5.3.1	Introduction.....	49
5.3.2	Development of the Feedforward Component .....	49
5.3.3	PID+ENFF Results .....	51
5.4	Smoothing.....	55
5.4.1	Introduction.....	55
5.4.1	Results.....	55
5.5	Interaction Problem and its Solution.....	58
5.5.1	Introduction.....	58
5.5.2	Interaction Problem .....	58
5.5.3	Solution.....	60
5.6	Mitigation of Valve Stiction .....	62
5.7	Windup Prevention Using Integral Bounding .....	63
5.7.1	Introduction.....	63
5.7.2	Solution.....	64
5.7.3	Results.....	65
5.8	Alternative PID .....	67
5.8.1	Introduction.....	67
5.8.2	Preliminary Results.....	69
5.9	Extended PID Controller .....	72
5.9.1	Introduction.....	72
5.9.2	Results.....	73

5.10	Detailed Quantitative Comparison.....	76
5.11	Conclusion .....	78
Chapter 6.	Conclusion .....	80
6.1	Summary and Achievements .....	80
6.2	Future work.....	82
Reference.....		85
Appendix A: Setpoints Used in the Experiments.....		89
A2 : Multistep setpoint.....		90
A3 : Cosine .....		90
A4 : Fast ramp .....		90
A5: Slow ramp. ....		90
Appendix B: Additional Experimental Results .....		91
B1: PID.....		91
B1.1 Fast Ramp .....		91
B1.2 Slow ramp.....		93
B.1 PID+ ENFF .....		94
B2.2 Fast Ramp .....		94
B2.2Slow ramp.....		95
Extended PID .....		96
B3.1 Fast Ramp .....		96
B3.1 Slow ramp.....		98
Alternative PID .....		99
B4.1 Fast ramp .....		99

Slow Ramp.....	101
Appendix C : Tabulated results .....	102
C1: PID.....	102
C2: PID+ENFF .....	103
C3 :EPID .....	104
C4 : APID.....	106

**TABLES**

Table 1 Comparison of PID vs. PID+ENFF performance for the multi-step setpoint. 52

Table 2 Comparison of PID controller performances for unsmoothed and smoothed 35 PSI step setpoints. 57

Table 3 PID performance metrics. 77

Table 4 PID+ENFF performance metrics. 77

Table 5 EPID performance metrics. 78

Table 6 APID performance metrics. 78

**FIGURES**

- Figure 2.1 Demonstration of the Solidification Front 17
- Figure 2.2 Demonstration of Conflicting 'Chill Zones' 18
- Figure 2.3 Simplified demonstration of solidification scheme for a rectangular plate that represents the automotive component geometry.  
18
- Figure 3.1 Schematic diagram of the apparatus design 22
- Figure 4.1 Demonstration of the delay due to stiction. 33
- Figure 4.2 The slowly changing valve control voltage used to measure the quasi-static nonlinearity. 37
- Figure 4.3 Pressure response to the slowly changing valve control voltage shown in Figure 4.2.38
- Figure 4.4 Pressure vs. valve control voltage curves for a nozzle with a 50 degree fan angle, 0.5 GPM @ 40 PSI (1.89 L/min) flow rating.38
- Figure 4.5 Pressure vs. valve control voltage curves for a nozzle with a 50 degree fan angle, 2 GPM @ 40 PSI (7.57 L/min) flow rating. 39
- Figure 4.6 Pressure vs. valve control voltage curves for the final design of two 2 GPM nozzles per valve. 40
- Figure 5.1 PID controller block diagram for one subsystem of the plant.  
43
- Figure 5.2 PID controller pressure response and error for a mult-step setpoint. 45
- Figure 5.3 PID controller pressure response and error for a cosine setpoint.  
47
- Figure 5.4 PID Slow ramp Response 48
- Figure 5.5 Feedforward data and fitted ENFF equation. 50

Figure 5.6 PID+ENFF controller block diagram for one subsystem of the plant. 51

Figure 5.7 PID+ENFF controller pressure response and error for a multi-step setpoint. 53

Figure 5.8 PID+ENFF controller pressure response and error for a cosine setpoint. 54

Figure 5.9 PID+ENFF controller pressure response for an unsmoothed 35 PSI step setpoint. 56

Figure 5.10 PID+ENFF controller for the smoothed version of the step setpoint from Figure 5.10. 57

Figure 5.11 Pump curve for the HSC-20 pump used in the apparatus. 59

Figure 5.12 and Figure 5.13 Left: Pressure setpoint, response and error for 1<sup>st</sup> subsystem. Right: Pressure setpoint, response and error for 2<sup>nd</sup> subsystem. 60

Figure 5.15 Results produced for subsystems 1 and 2 using higher integral gains. 61

Figure 5.16 Block diagram of the PID+ENFF controller with integral bounding for one subsystem of the plant. 65

Figure 5.17 Pressure response for PID+ENFF controller without integral bounding. 66

Figure 5.18 Response for PID+ENFF controller after integral bounding. 67

Figure 5.19 APID controller block diagram for one subsystem of the plant. 68

Figure 5.20 APID controller pressure response and error for a multi-step setpoint. 70

Figure 5.21 APID controller pressure response and error for a cosine setpoint. 71

Figure 5.22 EPID controller block diagram for one subsystem of the plant.  
72

Figure 5.23 EPID controller pressure response and error for the multi-step setpoint. 74

Figure 5.24 EPID controller pressure response and error for the cosine setpoint. 75

**Abbreviation**

APID	Alternative PID
EPID	Extended PID
ENFF	Empirical Nonlinear Feedforward
NewCast	An internal project name
PID	Proportional plus Integral plus Derivative
PWM	Pulse Width Modulation

**Nomenclature**

<b>Symbol</b>	<b>Definition</b>	<b>Units</b>
$e_j(t)$	Pressure error	PSI
$j$	Current valve number	n/a (integer)
$k$	Current time step	n/a (integer)
$K_{p,j}$ , $K_{I,j}$ and $K_{d,j}$	PID gains	Volts/PSI
$P_{Des,j}$	Pressure	PSI
$P_j(t)$	Measured pressure	PSI
$T$	Timestep	ms
$t$	Time	ms
$t_k$	Discrete timestep	
$U_j$	Valve command voltage	Volts
Functions		
$f()$	Feed forward function	Volts
$sat ()$	Saturation function	PSI · s

***CHAPTER 1. INTRODUCTION***

The North American automotive industry have been continually striving to lower the curb weight of passenger automobiles in an effort to improve the gas mileage and reduce the amount of greenhouse gas emissions. CAFE (Corporate Average Fuel Economy) (United States Government 2010) standards mandate North American Automotive manufacturers' to improve gas mileage every year; not only for individual cars, but for groups of cars a manufactures produce; the fleet mileage. Reducing the curb weight of the passenger automobiles leads to significant reduction in average fuel consumption.

The strategy of this project is to develop a novel casting technology to enable the near net shaped casting of automotive components using the high performance Al and Mg alloys which have traditionally been used for manufacturing high strength wrought products. The success of this technology would enable a significant improvement in the mechanical and performance properties of the cast component. This will enable them to be used as high integrity structural parts in a passenger automobile. By replacing several of the high density Ferrous alloy components; this leads

to a significant improvement in the strength to weight ratio of the parts and result in a reduction in car mass.

As proof of concept, a structural automotive component is being used in this project to demonstrate the casting technology termed "NewCast". Where in the component is cast using a sand mould consisting of a water soluble binder which would be precisely demoulded using critically controlled water jets at various ranges of momenta. The ability to solidify the new alloy families of Al and Mg at significantly high cooling rates from the liquid state enables the alleviation of Hot Tearing during solidification and enables high levels of grain refinement. This is required to improve mechanical properties.

Hot tearing is a casting defect prevalent in Aluminium and Magnesium casting. This defect can damage near-net-shaped casting and is the biggest hurdle to casting these alloys and to this project.

The Automotive Sample Component used in this project is thin walled part; the aspect ratio of length to width is also greater than 10. This makes this part one of the most technologically challenging components to cast. Due to the long distance metal must travel and the rate at which it cools

Presently the component is manufactured from steel using a specialized stamping process and is very thin. The thickness of the component has been doubled to enable the substitution of this part with Al and Mg alloys. Mg and Al alloys have lower strengths but lighter weight leading to a larger volume lighter part.

The aim of this MASc thesis is to build the apparatus, and develop the custom control system to enable the precise water jet system to demould and quench this part.

## 1.1 NUCAST TECHNOLOGY

In the NewCast process, the liquid metal alloy is poured into a sand mould which consists of a water soluble sand binder system. When the alloy fills the cavity, a series of sequential water jet system is precisely timed to predictably cut through the sand mould. This is timed so that the moment the water jet touches the solidifying liquid alloy; solidification is about to occur naturally. This is so that the natural solidification rate is enhanced, so that the part can withstand the force of the impact, but before any errant solidification behavior can occur. This needs to be staged such that only one solidification front forms, or if multiple

solidification fronts form they are forced to collide in sacrificial zones; such as the sprue, runner or risers.

The mechanism of directly quenching a solidifying liquid alloy with water jet, is conceptually similar to the quenching and cooling methods employed in direct chill (DC) casting of ferrous and non-ferrous ingot and / or billets. The difference would be the significantly smaller "thermal inertia" in the NuCast process when compared to the requirements of steel DC castings (Flemings 1974) and (E. Doege\* 2001) and (RICHARD A. HARDIN 2002). The smaller thermal inertia is a combination of a lower density, a higher thermal conduction rate, and a lower thermal capacity per mass. These combine to shorten the window of solidification from minutes; to milliseconds.

The water jets in the NuCast process serve two purposes: the controlled removal of the sand mould in specific locations followed by the quenching of the solidifying liquid alloy: the one parameter, jet momentum will have to be controlled dynamically throughout the process to succeed. This controlled jet momentum influences the sand removal rate and the cooling rate of the solidifying metal.

The empirical equation of sand removal was developed by another module of this project as a part of the MASc thesis by Mr. Aykut Dursun. This provides the necessary understanding of the sand removal process. The rate of cooling and solidification interaction will be provided by a third module of this project, carried out by Mr. Satyam Sharma as a part of his MASc thesis.

There are two salient challenges posed by the NuCast technology for the development of a valid control system:

1. When the liquid metal is poured into the sand mould, it begins to cool rapidly because of the very thin walls and very high aspect ratio. To enable a successful casting, the water jet would have to impinge the liquid metal at the earliest possible time during solidification to enhance the grain refinement and mechanical properties of the cast part. However, if the momentum of the water jet impinging the solidifying liquid is too high then the jet would impart surface defects on the solidified part and render it useless. Hence, there is a critical time at which a water jet with a precisely controlled momentum impinges the solidifying components to enable a sound casting: this critical time is determined as a balance between the lowest fraction solid of the solidifying alloy at the time

of impingement by the water jet and highest possible jet momentum to effect the maximum heat removal during quenching/solidification.

2. The other process served by the water jet is the controlled removal of the sand mould at specified locations. The aim would be to expeditiously and predictably remove the sand mould by a jet while varying the jet momentum from high values in the beginning of the demoulding to lower values dictated by the requirement of the solidifying metal during the first jet impingement. An existing empirical equation predicts the time of demoulding as a function of thickness for various values of jet momentum and this serves as an input for designing the control system. The timing through the sand mould is based on the critical point in the material properties where the part is solidify.

This project aimed to design and develop a control system (hardware and software) that would overcome the two challenges mentioned above and validate the same.

## 1.2 ORGANIZATION OF THIS THESIS

The purpose of this thesis is to develop a sprayer control system for a rapid Aluminum/Magnesium casting process required to manufacture high strength light metal parts using the NuCast technology. The relevant background literature will be reviewed in Chapter 2, Chapter 3 will present the design of the apparatus, and Chapter 4 includes the behavior, physical parameters and logistics of the plant and its implications towards controller design. Chapter 5 will describe the progressive development and testing of the controller from a basic Proportional, Integral, and Derivative (PID) controller to an Extended PID controller capable of handling this challenging system. Chapter 6 will present the conclusions of this project and recommendations for the future.

## ***CHAPTER 2. LITERATURE REVIEW***

### ***2.1 INTRODUCTION***

The largest hurdle in this project was a nearly complete lack of prior art; very little research has been done into this kind of casting system. In fact only one prior researcher (David Weiss et al 2011) has done any work on a similar process of using water to impinge a sand mould and rapidly cool a casting. Their paper is extremely preliminary containing only that, the process was successful, as backed up by evidence of a cast component and microstructure. From the images in their publication, they appeared to have been using an ASCO Redhat control valve for controlling the flow. However, no controls information was included, nor any information concerning the water sprayer system.

The next difficulty is the lack of any appreciable background literature on control systems for the unique combination of high velocity, high flow rate, low pressure (compared to traditional hydraulics) hydraulic system. There are three uniquely separate fields of research that have been studied in tandem to develop the strategies for a valid control system in this project: the direct quenching of solidifying liquid alloy in Direct Chill (DC) casting which is relevant to the spraying and the quenching aspects

of the NuCast project. Processes in agricultural engineering involving development of control systems for spraying but usually involve very simple controllers and thirdly, literature on the control of hydraulic and pneumatic actuators for advanced control systems, but rarely envelope the parameter space required for the NuCast process. These have been elaborated in the subsequent sections of this Chapter.

## 2.2 SPRAY COOLING OF MATERIALS

(W. V. Mudawar 1989) and (I. Mudawar and WS.Valentine 1989) are two linked papers concerning the quenching of aluminum components, this is one of the first papers concerning the precision spray cooling of aluminium parts. Unlike the process being studied in this thesis, their primary motivation was the rapid cooling of *wrought parts*; parts that have left a die, a stamping machine or other heat treatment. This is conceptually similar to the NuCast technology wherein water jet is used to quench a solid component rather than a solidifying component. Rapid cooling of wrought alloys allows for the development of high material properties, regardless of any further heat treatment. Due to the hardware limitations, most of their experiments were isothermal and done on copper targets treated to behave similarly to the aluminium part. The

copper part was required because isothermal experiments at high temperatures with aluminium will cause the part to oxidize to the point that the results do not represent the actual parts. They also conducted transient aluminium quench experiments to confirm the results from the copper targets; this data is less prolific compared to the steady state experiments, as the aluminium parts would be scrapped due to corrosion. (W. V. Mudawar 1989) Did not change the sprayer flow rate during the process as this was not required for their research objectives. They also did not specify the type of valve that was used: it is likely that it was a manual globe or ball valve.

In contrast to light alloy quenching, another application of precision cooling is the spray quenching process that is performed during the continuous casting of steel. This process is used when making large billets of steel for mass production, transport, or for raw material for forgings. A large continuous stream of steel is poured into a bucket and extruded through a water-cooled exit, to quickly cool the outside. From there, this hot semisolid 'sheet' of metal is pulled into shape and rapidly cooled (for steel) through direct water jets and water-cooled rollers. The paper by (RICHARD A. HARDIN 2002) presents a simulation of the thermal profiles of this steel process, and then verifies with the real

process. There are numerous differences between quenching of steel in continuous casting and the NuCast process. Steel is a very dense, low conductivity metal which has a very large solidification range of over 700 K and time of solidification. Al and Mg alloys are light, highly conductive metals which can solidify in milliseconds through a narrow solidification range of about 100 K. These impede the direct translation of the control system requirements from the continuous casting process to the NuCast technology.

### **2.3 CONTROL OF AGRICULTURAL SPRAYERS**

Locating information on high flow rate, low pressure sprayer controls was very difficult because most hydraulic controllers are high pressure, and most sprayers are low pressure. However, one related area of research belongs to the agricultural industry, wherein, for decades, been reducing the usage of various pesticides, herbicides and fertilizer by developing advanced controllers to selectively spray individual plants and locations in the field.

The paper by (M.E.R Paice 1996) provides an exhaustive study of the various spraying, and droplet dispersion methods (not all involving sprayers). They also studied the types of valves and the advantages and

disadvantages of each. They concluded that pulse width modulated (PWM) on/off solenoid valves and proportional solenoid valves are the most ideal styles, since they are fast, precise and capable of a wide range of flow rates; even the ones required in the NuCast process.

A second agricultural paper (Escolà 2013) is concerned with timing the sprayer jets to hit individual trees and modulate the flow based on the presences of a tree, and the thickness of the foliage. This is conceptually similar to the requirements of this thesis. However, their focus was not on the control system as reflected by the minimal documentation on the design and style of their controller. Their open-loop controller was a simple 5<sup>th</sup> order polynomial applicable over narrow range of flow rates 0 to 1.32 GPM.

## **2.4 CONTROL OF WATER HYDRAULIC AND PNEUMATIC ACTUATORS**

The difficulty with low pressure hydraulics is that it is not a common subject. In addition, water hydraulics are subtly different from traditional oil hydraulics. The following three papers are demonstrations of how fluid powered actuation will be useful to understand the process of low pressure, high speed water jet sprays.

Water hydraulics is an interesting area of hydraulics research because this hydraulic fluid is environmentally friendly and non-toxic. Using water as an energy transfer mechanism in systems allows for a cheap and environmentally sound equipment. However, Hydraulic oil has been chemically designed to be the ideal hydraulic medium. It is designed to be noncorrosive; lubricating; and to have linear thermal and pressure behaviors. Water is not popular since it has none of these properties. In fact, "it has many unknown parameters and strong nonlinearity such as friction in actuators and leakage flow in actuators and/or valves." (Tsuyoshi Yamada 2012).

The purpose of the paper by (Tsuyoshi Yamada 2012) is to show that precision control of a water-based hydraulic system is feasible. They demonstrate this through simulations and experiments. They design and compare the performance of simple adaptive controller, a model reference adaptive controller, and a PI controller. They conclude that even though the material properties of water are less understood, the system could be controlled. Their system is very small, they use a proportional spool valve to control a hydraulic cylinder with a 30 mm bore and 300 mm stroke loaded horizontally. The maximum flowrate of their system was 0.0188 L/s. This is very different to the system studied in the NuCast process,

only a transient force is required to accelerate the load. (Tsuyoshi Yamada 2012)

In contrast to the previous paper, the paper by (Harri Sairiala 2002), has a large flow rate system: the cylinder they used is similar in size to (Tsuyoshi Yamada 2012), and the highest flow rate was 0.5 L/s (7.9 Gpm). (Harri Sairiala 2002), used a simple integrator with feedforwards component to control their system.

The final paper, a pneumatic controller for a rotational arm seems far from the hydraulic spraying controls that the NuCast process demands. However, several interesting parallels can be drawn from (Majed (Marv) Hamdan 2000), wherein, although the work concerned a pneumatic system, several parallels could be drawn between the pneumatic and hydraulic systems. The critical information from this publication's conclusion is the success of the combination of a feedforward and PID controller, to control the hysteresis. Traditionally a PID cannot control a nonlinear system acceptably. This is similar to the system being controlled and this is presented and documented in the Chapter 4 of this thesis document.

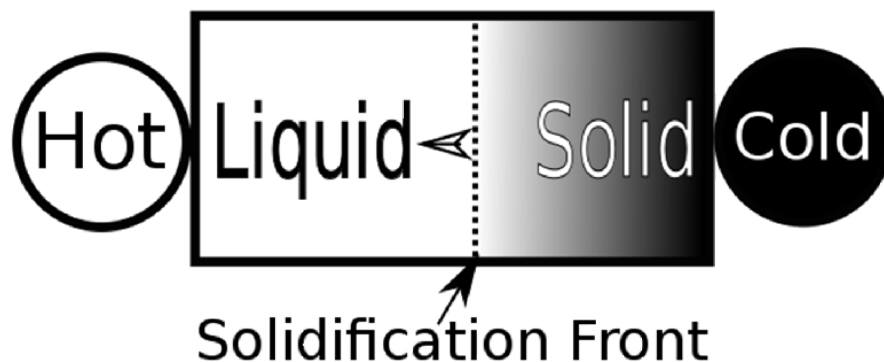
## **2.5 BOTTOM COOLING AND COOLANT ACCUMULATION**

The aim of the NuCast process is to maximize the rate of extraction of heat flux and the quantity of heat flux removed per unit time using the water jets. When the velocity of the water jet is coincident with the direction of gravity, the water will begin to accumulate between the impinging jet and the solidifying part and form a detrimental barrier to effecting quenching of the part. One simple method to circumvent this problem is to ensure that the effective water jet velocity is against the direction of gravity and hence, prevent pooling. This pooling behavior was documented in (Nitin Karwa 2012) and the improved effectiveness of using the water jets against gravity was confirmed by (Dursun n.d.) in his recent MASc thesis.

## **2.6 SOLIDIFICATION FRONT AND CASTING FLAW BEHAVIOR**

The following is a well understood concept to any casting engineer, but leads to difficulties for the controls of this system. All information is derived from (Flemings 1974) and class notes on solidification process by Dr. Sumanth Shankar at McMaster University in his course titled Fundamental of Solidification Processing (Shankar 2013).

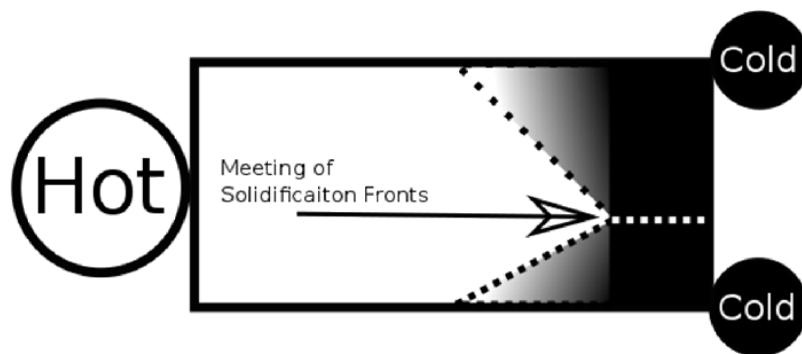
During solidification the metal must solidify from one point to another in a smooth, continuous manner. Naturally metal solidifies from the coldest side, the 'chill zone', to the hottest side, the sprue / risers or the location where metal enters the mould. As shown in Figure 2.1, when liquid metal solidifies it forms a 'solidification front' at the Solid / Liquid interface. This solidification front is ultimately what the materials engineers wish to control. In this project this 'chill zone' is formed through spray jet cooling. Unlike other methods of casting, this project allows us to vary the intensity and location of cooling by controlling the jets; this allows modulation on how the solidification front will move through the casting.



*Figure 2.1 Demonstration of the Solidification Front*

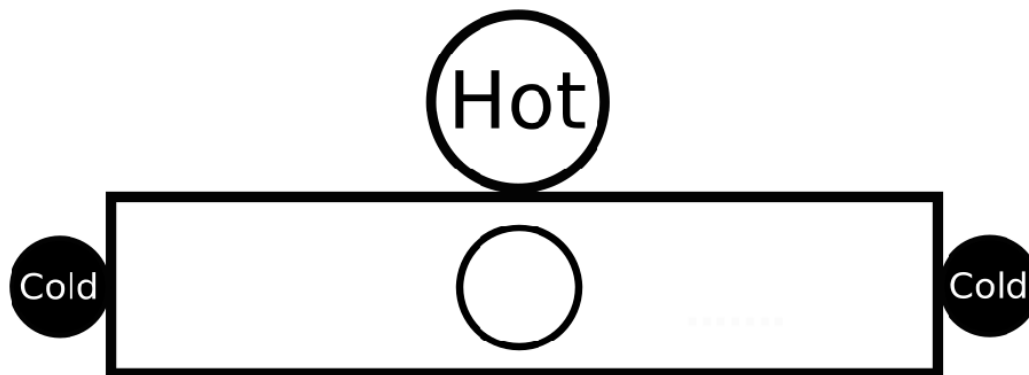
When two solidification fronts collide within a component during solidification, casting defects such as shrinkage and hot tearing tend to form and render the part ineffective. There is a volumetric contraction when liquid transforms to solid and this contraction is fed by the liquid from the hot side of the casting to maintain the integrity of the solidified part. When two fronts meet, the path between the bulk liquid and the solidifying front is significantly reduced or severed and this leads to shrinkage cavities and subsequently hot tearing in these regions.

Figure 2.2 shows a schematic of the result of two solidification fronts impinging on each other during solidification. It is imperative that a single solidification front be maintained from the initiation location of jet impingement to the riser, gating or sprue. Those parts will be removed so casting flaws can occur within them.



*Figure 2.2 Demonstration of Conflicting 'Chill Zones'*

Figure 2.3 presents a schematic of a long rectangular component which is a good representation of the Automotive Sample Component studied in this project. The part in this figure contains one sprue (termed Hot) through which the liquid metal is poured to fill the cavity and two regions termed Cold where in the first set of water jets will impinge the part to initiate the rapid solidification.



*Figure 2.3 Simplified demonstration of solidification scheme for a rectangular plate that represents the component geometry.*

In Figure 2.3, the symmetry of the part and the location of the hot sprue dictates that two water jets will have to simultaneously initiate the solidification from the two ends termed Cold. Since, the aspect ratio of the part is very large and with a length of about 40 inches, one water jet on

either end of the part would not be able to provide the uniform rapid cooling throughout the component to ensure uniform grain size and mechanical properties. A series of symmetrically jets placed between the Cold and Hot section of the part in Figure 2.3 is necessary. These jets will be activated sequentially to follow the path of the solidifying front and maintain its velocity.

## **2.7 FELLOW RESEARCHER AYKUT DURSUN**

The M.A.Sc. thesis recently presented by Mr. Aykut Dursun (Dursun n.d.), a fellow graduate student in this project has presented an empirical model for the demoulding of the sand wherein the distance cut by the water jet with a constant momentum arising from a nozzle at a fixed stand-off distance from the sand mould has a linear dependence on the time of cut; the linear model alleviates some of the complications that could have arose in the dynamic control of the jet because a single constant high momentum could be used for cutting through the sand mould and subsequently switched to a low jet momentum at a predetermined location in the mould close to the solidifying metal to enable a successful impingement with the metal to avoid any surface defect.

## 2.8 SUMMARY

The information gathered from the background literature have proven useful:

- the decision to use a proportional solenoids was derived from (M.E.R Paice 1996), and confirmed once an appropriate valve was located
- (W. V. Mudawar 1989) was extremely valuable in designing the apparatus, the experiments and how to proceed with this project
- While direct data is impossible to pull from (Escolà 2013), this work hinted at the behaviours of the control system described in Chapters 4 and 5 of this thesis, and the difficulties in controlling this system in Chapter 5.
- Finally the three chosen actuator papers all share a commonality with each other and this system, the use of a large integrator in a PI with a feedforwards component. The feedforward component approximately controls the system while the large integrator adjusts the real time changes to the system. The proportional

control used in such a system is small and is principally used to make rapid quick changes.

In summary what was learned from the literature directed the use of a proportional or PWM solenoid actuated valve which will be nonlinear and have considerable stiction. A good starting controller suggested would be a PI controller with a feedforward component.

## **CHAPTER 3. APPARATUS DESIGN**

### **3.1 INTRODUCTION**

This chapter documents the logical process that led to the construction of the apparatus whose schematic is shown in Figure 3.1. The pump is a pre-existing Gould 2HP HSC-20. The justification for using stationary nozzles is presented in section 3.2. The NuCast process: the need for, and development of, the containment chamber; and selection of valves and pressure sensors are described in sections 3.3, 3.4 and 3.5, respectively.

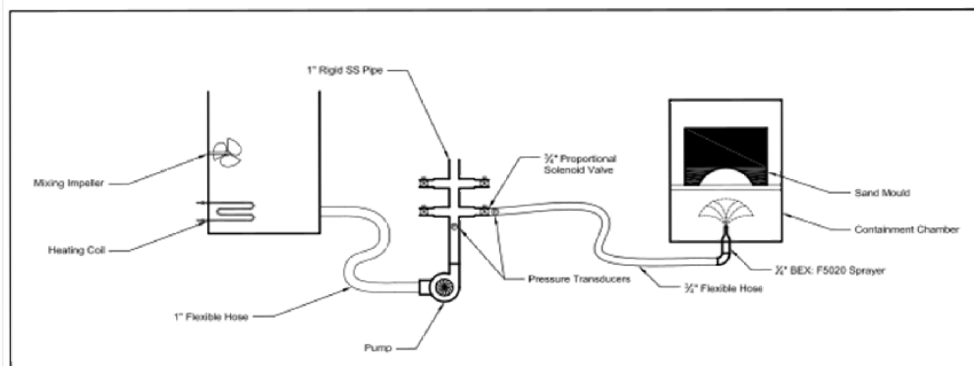


*Figure 3.1 Schematic diagram of the apparatus design*

### **3.2 JUSTIFICATION OF A STATIONARY SEQUENTIAL SPRAYER SETUP**

The underlying aim of creating a high integrity cast part, using the NuCast process, would be to maintain a uniform cooling rate during

solidification throughout the entire part. This mandates a dynamic control of the flow rate depending on the thickness of the location in the part being cooled by the jet. Thicker sections will require higher jet momentums to maintain a nearly uniform cooling rate and thinner section less. This is particularly important because thermal stress could develop when a part's thickness changes and the jet is unaltered.

The logical conclusion is to move the sprayer jet or part, and adjust flow rate based on the thickness of the part, adjusting the spray as you cover different sections of the part. Similar to an automatic spraypaint robot. However, moving the part cannot be done because it will agitate the semisolid and liquid metal. Due to what was previously stated in Chapter 2.4 the sprayers must be located under the part. Sadly, because of project constraints a moving jet underneath the part was not possible. The solution to this was a series of sprayer jets, adjusting the spraying rate to 'simulate' a moving wave of water, this is pushed the difficulty from a physical design of the system, to a controls problem of adjusting the jets.

This is why a controller is needed for this project. The solidification front travels extremely quickly and the sprayers must keep pace with it. This is too fast for manual control.

### 3.3 CONTAINMENT CHAMBER

The possible malfunction of the NuCast process and the perils of the water jet directly interacting with liquid metal at high temperature mandated a closed chamber for the NuCast process. Further, the chamber contained the several high momentum water jets and the mixture of water and demoulded sand in the process. The chamber also acted as a sedimentation tank for the demoulded sand in the bottom while releasing the water through an outlet at an elevated location.

Operator Health and Safety protocols necessitated by the use of high temperature liquid Al and Mg alloys in conjunction with water jets were of paramount importance in designing and implementing the chamber. There were sections of transparent polycarbonate sheets in the chamber for ease of visualization of the casting process. The peripheral hardware, such as the pump, water tank, controller and computer were placed outside the chamber. Several experiments were carried out to ensure the safe operation of the NuCast process within the chamber.

### 3.4 VALVE SELECTION

The valve selection for this project was mandated by the requirement of high flow rate (10 GPM max.), medium pressure (150 PSI), and fast response time (less than 20 ms). This presents a rather unique combination of valve requirement seldom observed in commercial operations or literature. Since, the project only aims to provide a proof of concept of the NuCast process technology and the development of the suitable sand and binder system. predictability of the cutting of the sand mould by water jets and the development of the control system was carried out in tandem over a two year period, this system was designed to a 'best possible' standard. The solenoid actuation was selected and directly based on the work by (M.E.R Paice 1996); the cost of the project coupled with the time constraints presented by the project deliverables also influenced the selection of the valves.

#### *3.4.1 Pulse Width Modulation Valves*

One option for valve selection is the Pulse Width Modulation Valve, or valves which modulate the flow through them by rapidly opening and closing. This option is capable of highly precise control and extremely fast. The disadvantage is that it is very noisy. Audio, electrical, and water

output will be pulsating. There were no valves available within the budget, flow requirements and pressure ranges requirements mandated by this project. The PWM option was unable to be explored. In future expansions of the NuCast project, it is recommended to use the PWM valves as substitutes for the proportional flow control valves used in this project.

### ***3.4.2 Proportional Solenoid***

Proportional solenoid works by using an electrical solenoid coils to exert force on the mechanical plunger which is countered by a spring. This allows a fractional force to be applied to the plunger to alter the orifice size, thus altering the flow rate and pressure drop; allowing for a proportional flow control valve. The rate of change on this proportional solenoid is fast; the valve can reliably resolve motion in 5-10 ms depending on the 'distance' of the motion. In practice this is slightly slower because the controller needs to 'check' to make sure the system is actually reaching the point (flow) it is supposed to. Although the valve may open quickly, the water flow will fail to respond with similar speed and some time lag will appear in resolving the flow pressure past the valve. Since the rate of change mandated by the NuCast process in this

project is about half a second, the time lag in flow adjustment would not pose a serious threat to the process control.

The valve selected was a EV206B from Danfoss Direct sized to 3/4 inch. While the North America distributor was problematic, this valve is extremely fast, precise, easy to control and ruggedly built. It is recommended that this valve be used in future work.

### **3.5 PRESSURE SENSORS**

This system is controlled primarily through a pair of pressure sensors for each valve: one before and one after the valve. The sensor before the valve is a common manifold pressure sensor shared by all the valves in the process. The accuracy from the manufacturer is 0.25% which includes linearity hysteresis and repeatability. This leads to a maximum error of 0.375 PSI (2.586 KPa) over the 0-150 PSI (0-1035KPa) range of the pressure sensor, and had a response time greater than the 1 ms operating speed of the data acquisition unit.

These pressure sensors were located as close to the valves as possible. This was done to reduce the transport delay between the valve and sensor; and to protect the sensors from corrosion. Transport delay tends to destabilize a control system and therefore should be minimized.

### 3.6 SYSTEM DESIGN AND PERIPHERALS

A large water tank was used to feed the system to ensure a constant supply of water with a minimum pressure head. The tank fed into the pump (Figure 5.12) with a 6 m, 0.019 m dia. Hose. The length of the hose posed the problem of water hammer during initial start up. The pump lead into a series of 4 way connectors, this acted as a manifold. The top of this manifold had a length of rigid pipe that was acted as an accumulator; the length could be adjusted to help damp vibrations from the pump. A schematic of the experimental apparatus is shown in Figure 3-1.

The pipe coming out of the manifold was immediately reduced to 3/4 pipe to accommodate the four (4) valves. The hose was fed into the containment chamber through flexible rubber hoses and rigidly fixed to the predetermined nozzle locations, respectively. The nozzle was attached to the end of each hose in the chamber and permanently fixed to the structure of the apparatus at pre-determined locations. Fixing the hose is actually very important as a feedback loop would occur otherwise; as the hose vibrates, the valve and controller could vibrate, this moving hose would gradually swell until the valve and the hose were thrashing in sync.

As previously mentioned, the pressure sensors are located at the base of the manifold, and past each individual valve. They are naturally located as close to the valves as possible, and at the base of the manifold, far enough from the pump to not be directly influenced.

### 3.7 SUMMARY

The physical design of the experimental apparatus, and choice of valves and pressure sensors would be able to control the system in the NuCast process to the desired pressures, flow rates, and timing requirements mandated by the process requirements. However these design decisions complicated the control system development. This issue is further discussed in Chapters 4 and 5.

**CHAPTER 4. PLANT BEHAVIOR****4.1 INTRODUCTION**

The term 'plant' refers to the dynamic system being controlled. This Chapter discusses the nonlinear behaviors of the hydraulic plant. In particular, it focuses on how the nonlinearity makes it very challenging to control at the pressures we wish to operate at.

**4.2 PLANT OVERVIEW**

As shown in Figure 4.1, the plant is a hydraulic system. A tank, pump, hose and manifold deliver pressurized water to three subsystems. Each subsystem consists of a proportional valve, pressure sensor, hose and sprayer nozzle. The valve may be approximated as a variable hydraulic resistor, the hose as a hydraulic inductor, and the nozzle as a nonlinear hydraulic resistor.

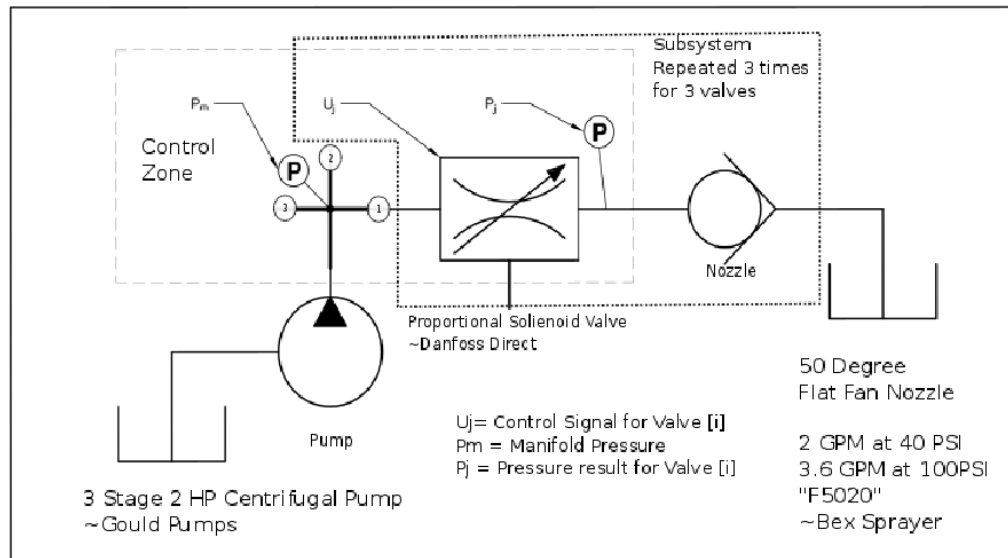


Figure 4.1 Block diagram of the plant.

### 4.3 CHALLENGING DYNAMIC BEHAVIORS

This plant experiences four dynamic behaviors which can dramatically affect a controller's performance, as will be discussed further in Chapter 5. These are the pressure noise, valve stiction, water hammer and quasi-static nonlinearity.

#### 4.3.1 *Pressure noise*

A problem implementing a controller with this system was the presence of noise in the pressure sensor measurements. Most of this was system noise (also known as disturbances) caused by the pump.

Additionally there was some electrical noise that added to this pump noise. The amplitude of the combined noise was about 0.1 PSI.

#### *4.3.2 Valve stiction*

Stiction in this system is made worse by the non-lubricating nature of water and the significant backpressure forcing the valve closed. The stiction in this system only occurs when the valve is first opened; this is because the only time two surfaces touch is when the valve is fully closed. Holding the valve open at a position does not result in appreciable stiction. However once the valve is closed, and the hose depressurizes, considerable force is needed to re-open it. This stiction adds a 400-600 ms delay (see Figure 4.2 for an example), and can be mitigated. This stiction is difficult but manageable. This stiction has the possibility of destabilizing a controller. This behavior and the solution will be discussed in section 5.6.

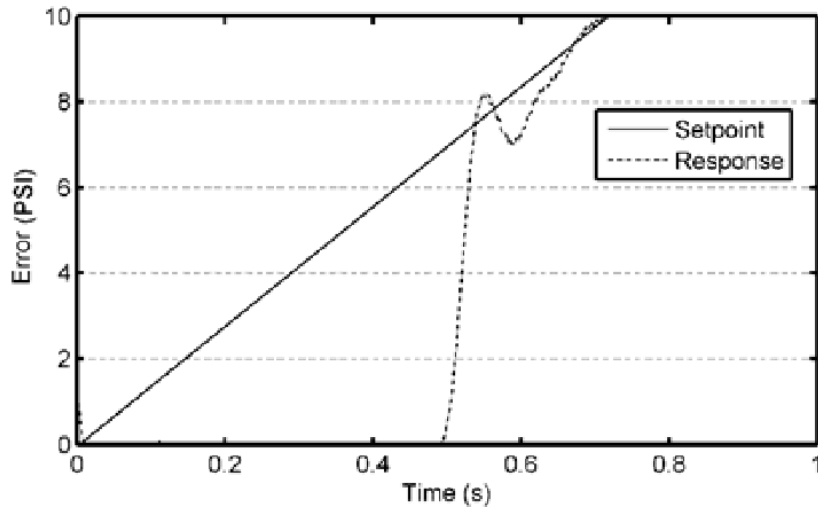


Figure 4.1 Demonstration of the delay due to stiction.

### 4.3.3 Water hammer

Water hammer is a phenomenon where suddenly changing the flow rate of a large mass of moving water will create potentially damaging transient pressure effects. In this system, the long hose (6 m, 0.019 m dia.) leading into the pump contains a large mass of water. Within the operation of this system there are two times when water hammer can cause problems. The first is when the valve is first opened. Because of the tendency of the hoses to empty between operations, air pockets form past the valve, causing a massive water inrush which hits the nozzle and reflects in a pressure shockwave back through the system. This is most

noticeable when the system is first turned on, but can be an issue if the valve is closed for any extended period.

The second time there is a problem is whenever a valve shuts. Whenever a valve quickly closed (fully or partly) and another valve is open the water flow that was formerly going through the open valve splits and redirects itself to the all other open paths. This sudden increase is received by the other plant subsystems as a disturbance and they react accordingly. The details of this problem are discussed in section 5.4.

#### ***4.3.4 Plant nonlinearity and its mitigation***

Friction, static or dynamic, is not the source of the dominant nonlinearity observed in this system. That nonlinearity is caused by an interesting combination of design requirements. Each nozzle is required to provide a powerful jet from a relatively low pressure source. This was accomplished by using large diameter hose (to reduce their hydraulic resistances) from the valve to the nozzle, plus a narrow nozzle with a very high nonlinear resistance. The resistance from the nozzle creates a large backpressure that was found to greatly affect the valve's quasi-static behavior.

The valve contains a spring and solenoid for actuating its needle. It was found experimentally that the needle's opening/closing behavior also depended on the upstream and downstream pressures. In quasi-static conditions the downstream pressure and nozzle backpressure are equal assuming the hose's resistance is negligible. Of course the needle's position also changed the valve's hydraulic resistance. This resistance change, in series with the nonlinear nozzle resistance, created an unusual quasi-static nonlinear behavior with hysteresis between the downstream pressure (that is being sensed, and will later be controlled) and the valve control voltage.

To study the quasi-static nonlinearity, the system was started and left running for a short time, then the valve was slowly opened. The voltage was ramped from 0 to 10 over a 250 s period, then ramping back down to 0 over another 250 s period as shown in Figure 4.2. Figure 4.3 shows the corresponding pressure response vs. time. Figures 4.4 and 4.5 show the pressure vs. valve control voltage curves for two different nozzles. Two significant nonlinearities are apparent in these results. First, there is a very large hysteresis between the valve opening curve of the right side and the valve closing curve on the left. The second nonlinearity is the changing slope of both the opening and the closing curves. With these two nozzles,

as the valve voltage was gradually increased, the pressure first increased slowly then suddenly increased at around 1.5-3.5 Volts, before returning to a gradual slope. The portion with the nearly vertical slope made precisely controlling this system almost impossible since a tiny change in valve voltage results in a very large pressure change. Naturally, the physical plant had to be improved until it could be controlled. Two significant changes were made. It was discovered that high flow rate nozzles produce more linear behavior than low flow rate nozzles, as is apparent by comparing the results in Figures 4.4 and 4.5. The curves for the 2 GPM @ 40 PSI nozzle have a smaller slope starting around 65 PSI. However this nozzle still contains a very steep section so this change was not enough to mitigate the difficulty of controlling this plant. For further improvement, it was realized that the flow rate needed to increase. One idea was to change to an even larger nozzle. The problem was that increasing the size of the nozzle would have removed too much sand, too quickly, and destroyed the solidifying component. Since the part is symmetrical, and the flow patterns will be symmetrical, the idea of putting two nozzles on one valve was proposed by Dr. Kifah Takrouri (Takrouri 2015). Two hoses and two 2 GPM nozzles were then connected to each valve, making a total of six nozzles. Note that using six 2 GPM nozzles nearly maxed out the pump's flow rate capacity. The resulting

pressure vs. valve control voltage curves are shown in Figure 4.6. This final design produced a dramatic improvement and resulted in lower sloped curves that are more symmetric. The reduction in slope was sufficient to allow a precise pressure controller to be developed.

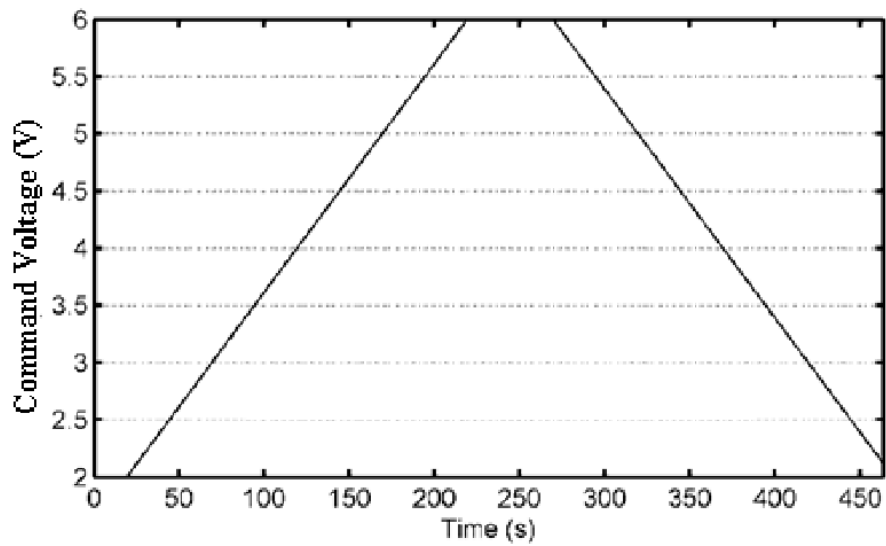


Figure 4.2 The slowly changing valve control voltage used to measure the quasi-static nonlinearity.

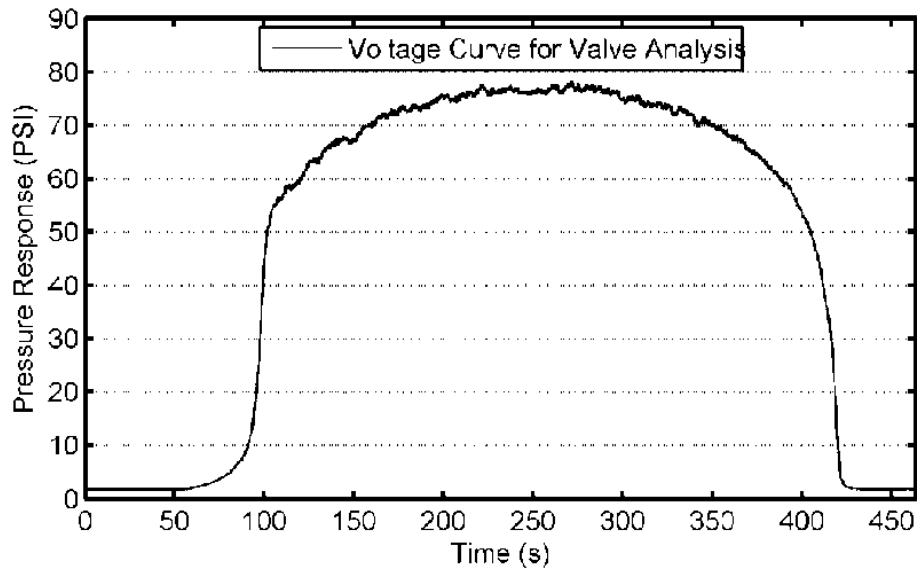


Figure 4.3 Pressure response to the slowly changing valve control voltage shown in Figure 4.2.

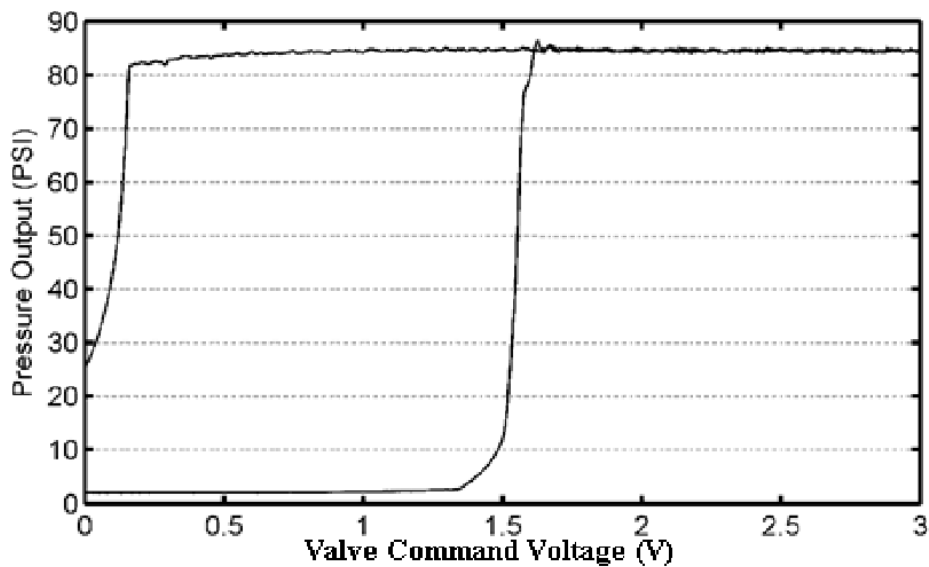


Figure 4.4 Pressure vs. valve control voltage curves for a nozzle with a 50 degree fan angle, 0.5 GPM @ 40 PSI (1.89 L/min) flow rating.

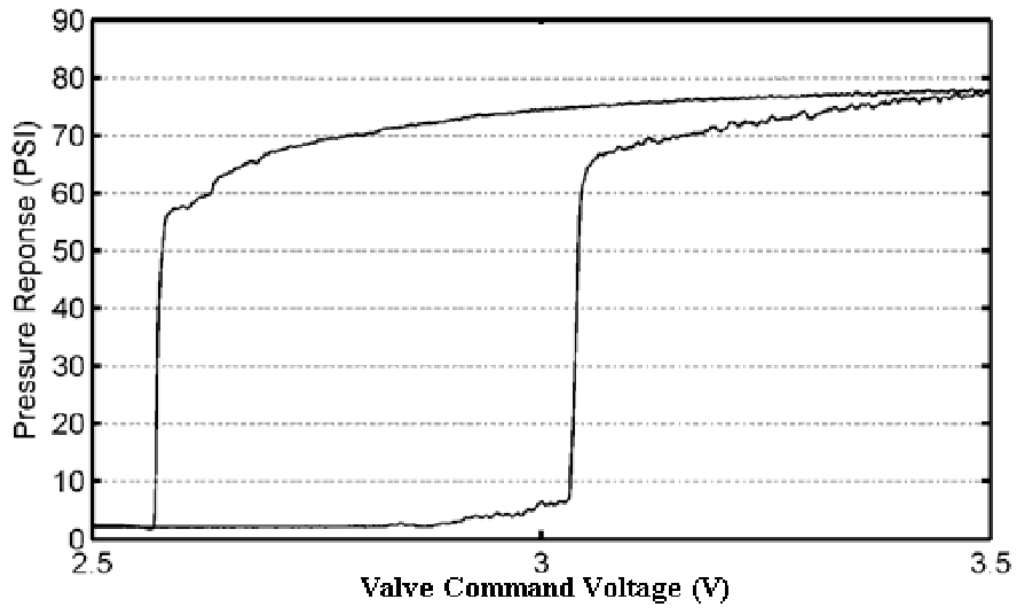
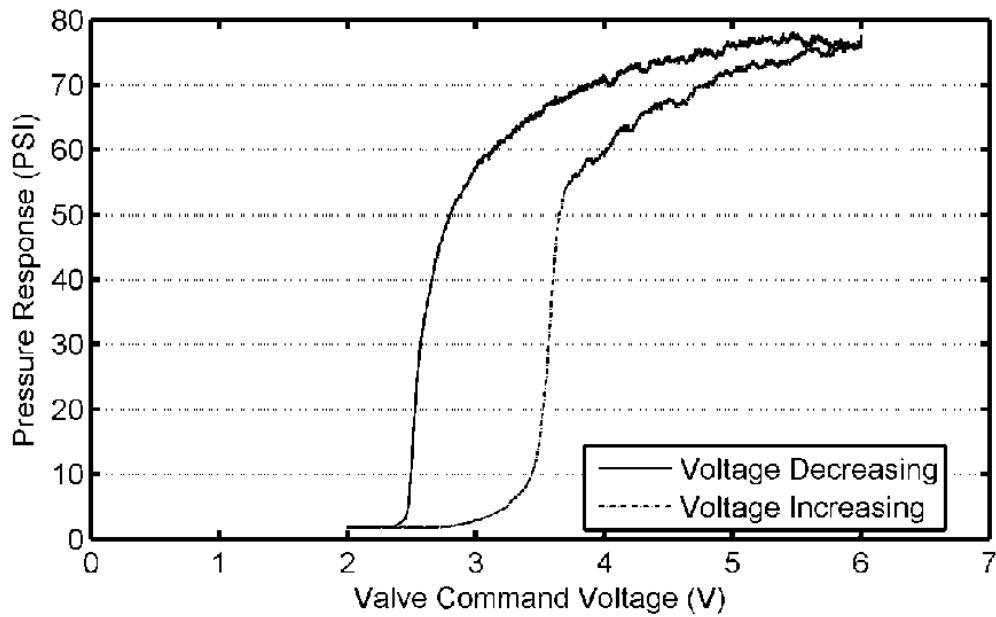


Figure 4.5 Pressure vs. valve control voltage curves for a nozzle with a 50 degree fan angle, 2 GPM @ 40 PSI (7.57 L/min) flow rating.



*Figure 4.6 Pressure vs. valve control voltage curves for the final design of two 2 GPM nozzles per valve.*

#### 4.4 CONCLUSION

Four behaviors of the plant which can make the control challenging were discussed in this Chapter. These are the pressure noise, valve stiction, water hammer and quasi-static nonlinearity. The pressure noise and valve stiction behaviors were relatively simple to solve during the controller development. The water hammer was also solvable except at the very beginning of each test when the hoses were not fully primed. While the plant's quasi-static nonlinearity was reduced in this Chapter it wasn't completely removed and required a special feedforward control term to be created. The details of the controller development and testing are presented in Chapter 5.

***CHAPTER 5. CONTROLLER DEVELOPMENT******5.1 INTRODUCTION***

Recalling Chapter 1, the purpose of the control system is to control the timing and flowrate of multiple jets by controlling the each nozzle's backpressure. As defined by the material properties, certain requirements for this system are stringent. It is required to make very fast flowrate changes, at precise times, in order to match the solidification requirements. In this system high speed actuations are required; this leads to large transient errors in the system. These transient errors are not a concern provided they are quickly reduced to a small steady state error. As determined by (Dursun n.d.) as much as a 2% steady state error is acceptable to this system.

This chapter presents the evolution of the controller developed in this thesis. By using the information presented in the previous chapter, a PID controller is extended through several design iterations to successfully control the plant. The setpoints used in the experiments are described in Appendix A. The design started with a classical PID controller. A feedforward compensator was then developed based on experimental data and combined with the PID controller. Next, smoothing was applied to the setpoint to decrease the overshoot at the expense of response time.

The interaction between the three subsystems was then studied and solved by modifying the integral term. The final version of the controller will be called an “Extended PID” (EPID).

Lastly, an alternate controller that involves putting a PID controller in series with the feedforward equations is proposed, and some preliminary results included. Those results suggest that it is worthy of further study.

## 5.2 PID CONTROLLER

### 5.2.1 *Introduction*

A natural first step is a PID control system. The PID is debatably the origin of modern control systems, first documented in the 1890's, and developed at the turn of the 1900's. Directly based on centrifugal governors and the behavior of helmsmen in boats, it was not fully discussed until (Minorsky 1922) “Directional Stability of Automatically Steered Bodies”. The PID controller's combination of the error, the derivative of the error, and the error integral; scaled by their respective gains; is now known to produce a surprisingly robust controller with a simple design. Additionally it is not very difficult to tune and a very popular ‘baseline’ controller. Finally, it is a computationally light controller allowing it to run at the high speed required for this project's timing needs.

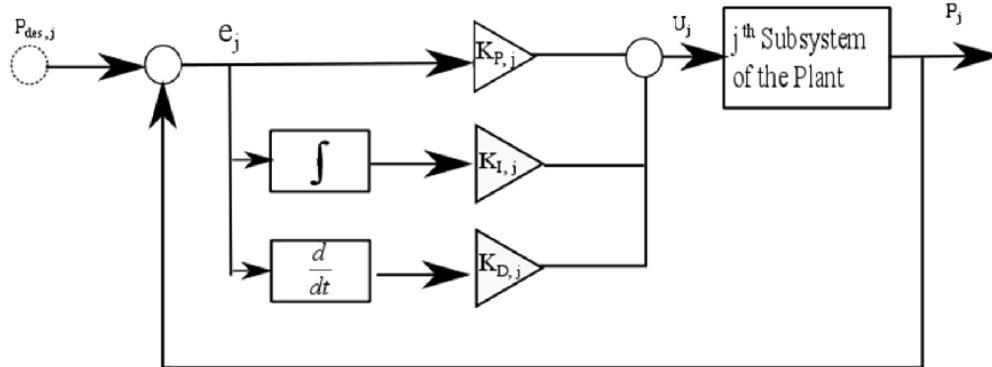


Figure 5.1 PID controller block diagram for one subsystem of the plant.

The PID controller's output (which equals the input to the subsystem of the plant) is the sum of the proportional, integral and derivative terms.

The corresponding block diagram for one of the subsystems is shown in

Figure 5.1. In continuous time the PID controller equation is:

$$U_j(t) = K_{p,j}e_j(t) + K_{I,j}\int_0^t e_j(\tau)d\tau + K_{d,j}\frac{d}{dt}e_j(t) \text{ and} \quad (5-1)$$

$$e_j(t) = P_{des,j}(t) - P_j(t) \quad (5-2)$$

where  $t$  is the continuous time;  $U_j(t)$  is the valve control voltage;  $e_j(t)$  is the pressure error;  $P_{des,j}(t)$  is the setpoint (i.e., the desired pressure);  $P_j(t)$  is the measured pressure;  $K_{p,j}$ ,  $K_{I,j}$  and  $K_{d,j}$  are the proportional, integral and derivative gains, respectively; and the  $j$  subscript indicates the variable

belongs to the  $j^{\text{th}}$  subsystem. In practice this will be implemented as a digital controller operating in discrete time. The discrete time version is:

$$U(t_k) = K_{P,j}e_j(t_k) + K_{I,j} \sum_{i=0}^k (e_j(t_i))T + K_{d,j} \frac{e_j(t_k) - e_j(t_{k-1})}{T} \quad (5-3)$$

where  $t_k$  is the current discrete time, and  $T$  is the time step (also known as the sampling period) of the controller. In the implementation, the integral term in (5-3) was reset to zero whenever the setpoint equalled zero.

### 5.2.2 *PID Results*

The response to the multi-step setpoint obtained using the PID controller is shown in Figure 5.2. Clearly, these results are unacceptable. There is an overshoot at 35 PSI of 42%, and the system takes upwards of 5 seconds to reach the correct steady state value at 80 PSI. This was the best result obtained by manual tuning. The PID required a large integral gain. This produced the slow response and large overshoots.

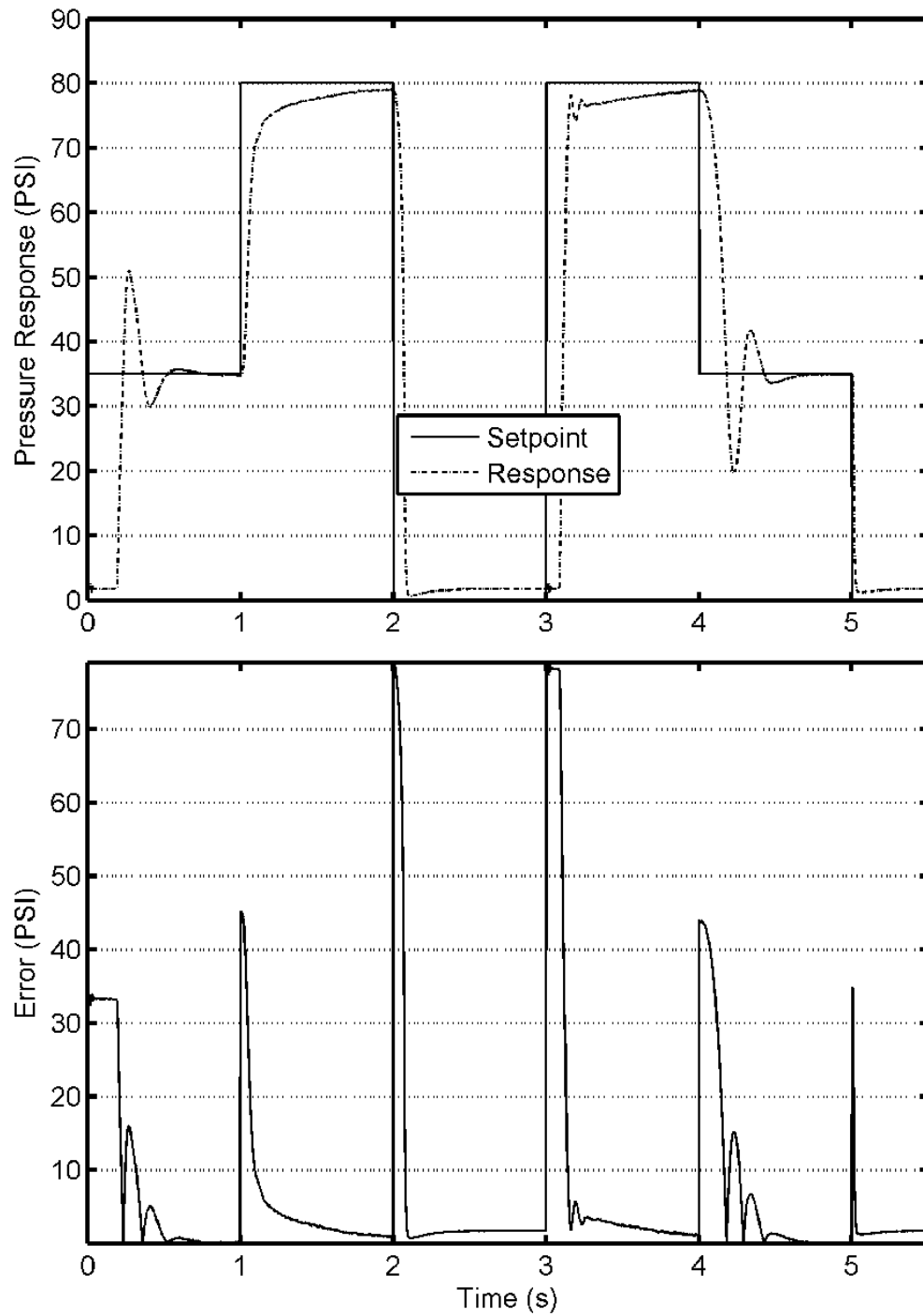


Figure 5.2 PID controller pressure response and error for a multistep setpoint.

The results for the cosine setpoint shown in Figure 5.3 demonstrate the serious difficulties the PID controller had with this plant. The controller slowly increased the valve control voltage and, due to valve's stiction, the pressure did not change until over 1 s after the setpoint began rising. The response then continues to lag far behind the setpoint due to a combination of the stiction and integral windup.

In comparison, the slow ramp tracking result shown in Figure 5.4 is fairly good, except for the transient error during the first second. After that the error was contained within a 5% boundary. This is still unacceptable since it exceeds the 2% error requirement.

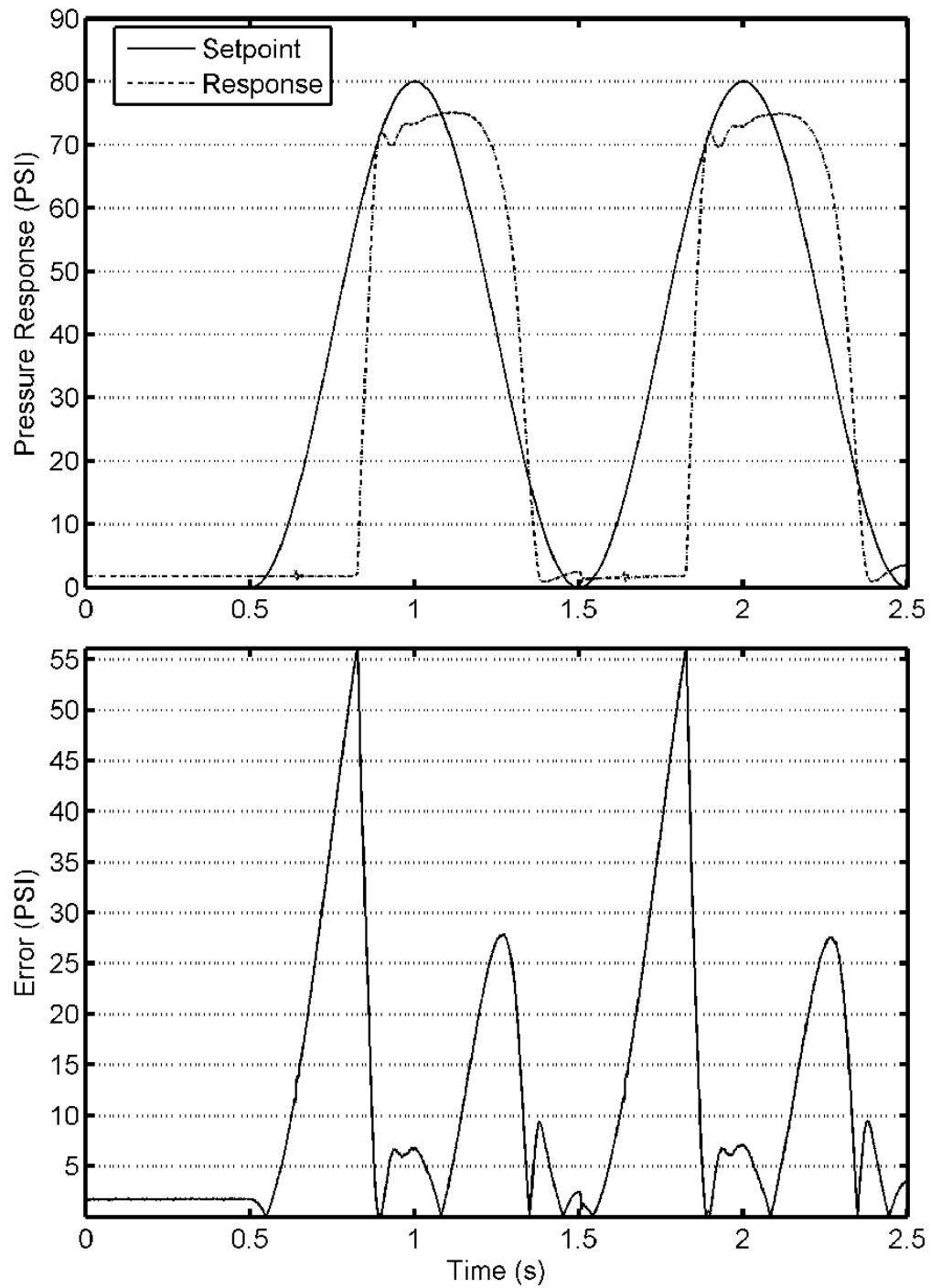


Figure 5.3 PID controller pressure response and error for a cosine setpoint.

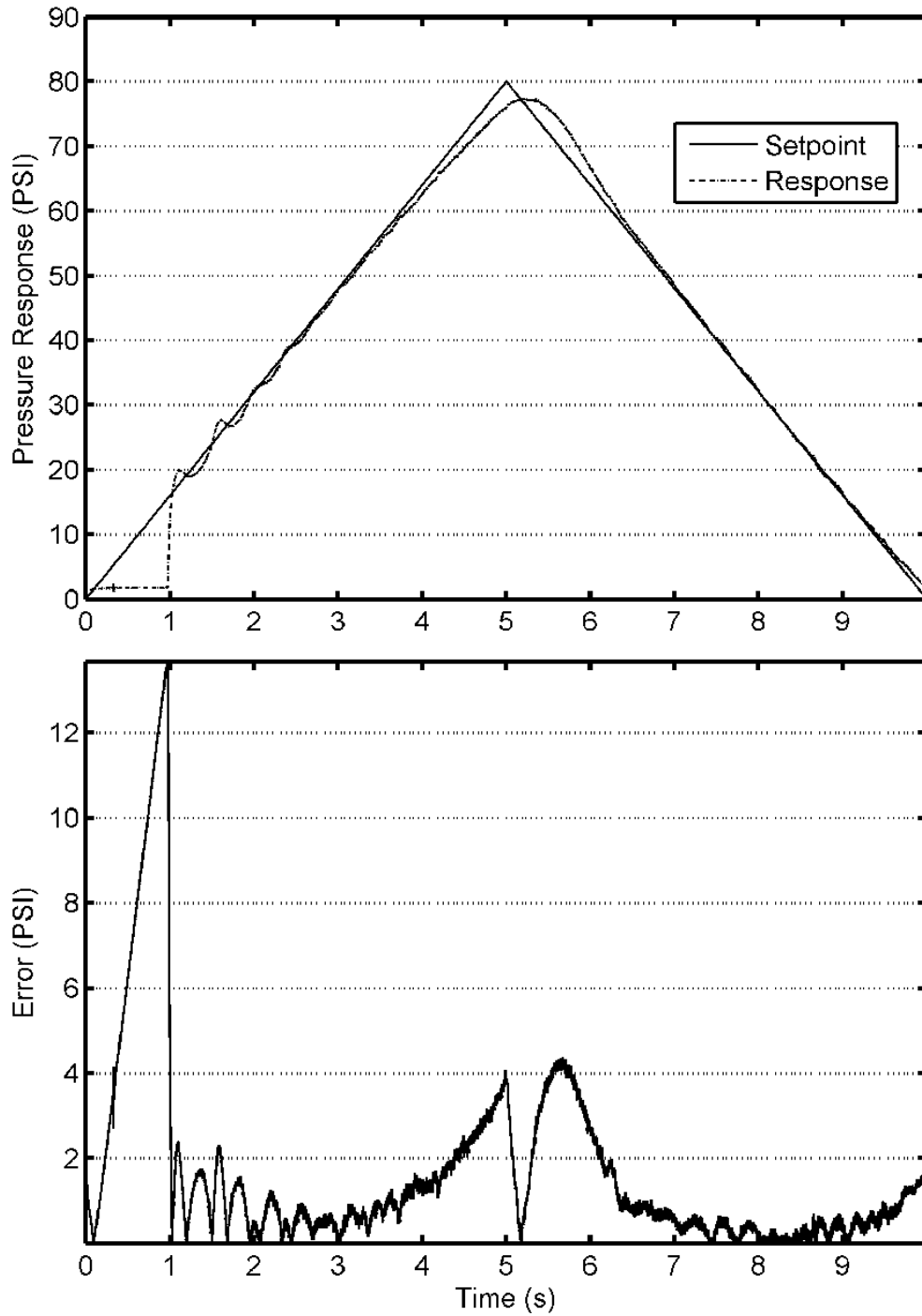


Figure 5.4 PID Slow ramp Response

### 5.3 DEVELOPMENT OF PID PLUS FEEDFORWARD CONTROLLER

#### 5.3.1 *Introduction*

Adding a feedforward component is done in many control systems to improve the setpoint tracking performance. A feedforward component may involve a simple gain or may be based on an inverse model. In this thesis the feedforward component is obtained from an inverse model of the plant's quasi-static nonlinearity. If the feedforward component was perfect then the quasi-static component of the setpoint would be followed perfectly and the PID feedback would only be required for the higher frequency errors. In reality the feedforward component will only approximate the average quasi-static behavior so the integral feedback is still needed to compensate for quasi-static errors.

#### 5.3.2 *Development of the Feedforward Component*

The data describing the quasi-static nonlinearity was collected for each valve as described in section 4.2.4. An example result was previously shown in Figure 4.6. The results for the other valves were similar. An empirical nonlinear feedforward (ENFF) equation was obtained by fitting the relationship between the pressure and the valve control voltage. To obtain the inverse model, the pressure was taken to be the independent variable and the valve voltage was the dependent variable. It was found

that the nonlinearity of the data could be approximated well by a 5th order polynomial equation. Higher order polynomials could be used to obtain more accurate results at the expense of extra computation. The raw data and fitted equation for one of the valves is shown in Figure 5.5.

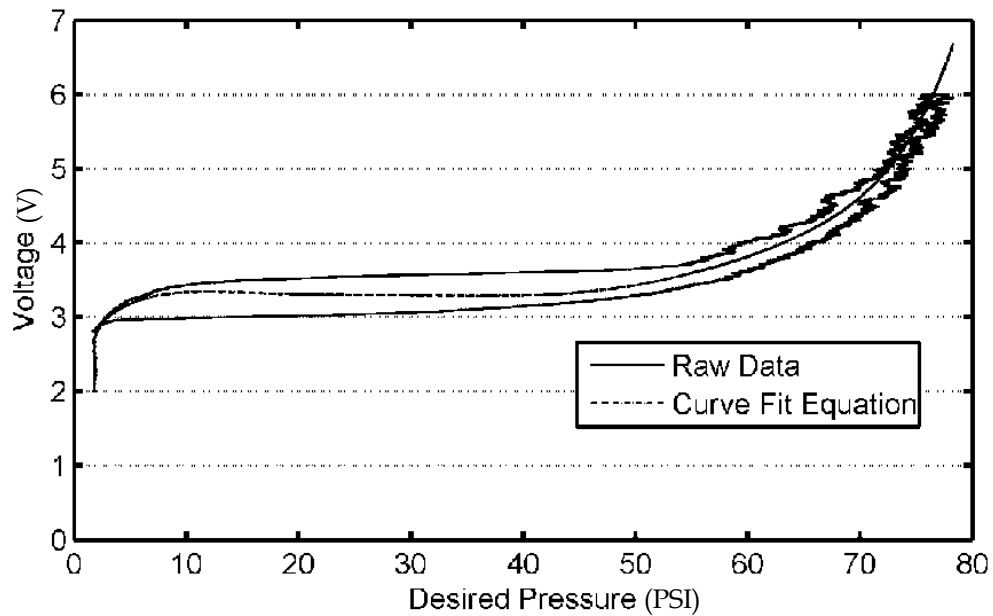


Figure 5.5 Feedforward data and fitted ENFF equation.

The block diagram for the PID+ENFF controller is shown in Figure 5.6.

In continuous time, its equation is:

$$U_j(t) = f(P_{des,j}(t)) + K_{p,j}e_j(t) + K_{i,j}\int_0^t e_j(\tau)d\tau + K_{d,j}\frac{d}{dt}e_j(t)$$

5-4

where  $f_j(P_{des,j}(t_k))$  is the ENFF equation for the valve used in the  $j^{\text{th}}$

subsystem. The discrete time version is:

$$U(t_k) = f(P_{des,j}(t)) + K_{P,j}e_j(t_k) + K_{I,j} \sum_{i=0}^k (e_j(t_i))T + K_{D,j} \frac{e_j(t_k) - e_j(t_{k-1})}{T} \quad 5-5$$

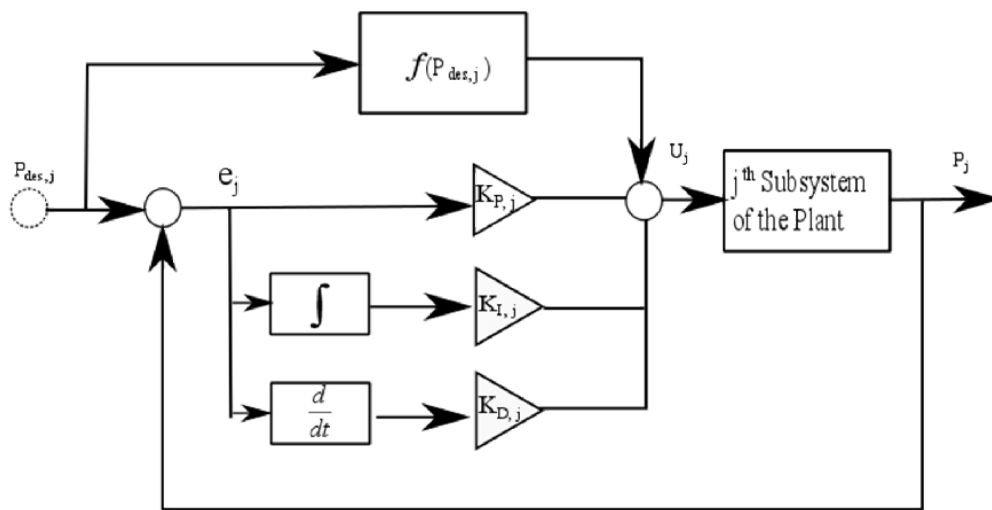


Figure 5.6 PID+ENFF controller block diagram for one subsystem of the plant.

### 5.3.3 PID+ENFF Results

Comparing Figure 5.2 to Figure 5.7, it is clear that adding the ENFF component greatly reduced the overshoot. The response is also slower as a result of retuning the gains. The quantitative performance comparisons will mostly use the following three metrics: mean error, mean absolute

error and maximum absolute error. Their values are listed in Table 1 for PID and PID+ENFF controllers and the multi-step setpoint. Using the PID+ENFF controller improved the mean error by 13% and the mean ABS. error by 26%. It also inverted the sign of the mean error because the ENFF equation was deliberately set to give an output that was slightly low. This causes the PID to always be pulling the control voltage slightly higher. This was done intentionally because if the flow rate is slightly low, the part will have inferior material properties when quenched. If the flow rate is too high the part will be damaged and possibly destroyed. A weak part is preferable to a failed one.

As shown in Figure 5.8, the cosine response was also improved compared to the PID result in Figure 5.3. However, even though the response is more cosine-like it is still significantly delayed relative to the setpoint.

*Table 1 Comparison of PID vs. PID+ENFF performance for the multi-step setpoint.*

<b>Controller</b>	<b>Mean error (PSI)</b>	<b>Mean Abs. Error (PSI)</b>	<b>Max. Abs. Error (PSI)</b>
<b>PID</b>	1.7	7.2	78.9
<b>PID+ENFF</b>	-1.50	5.3	70.7

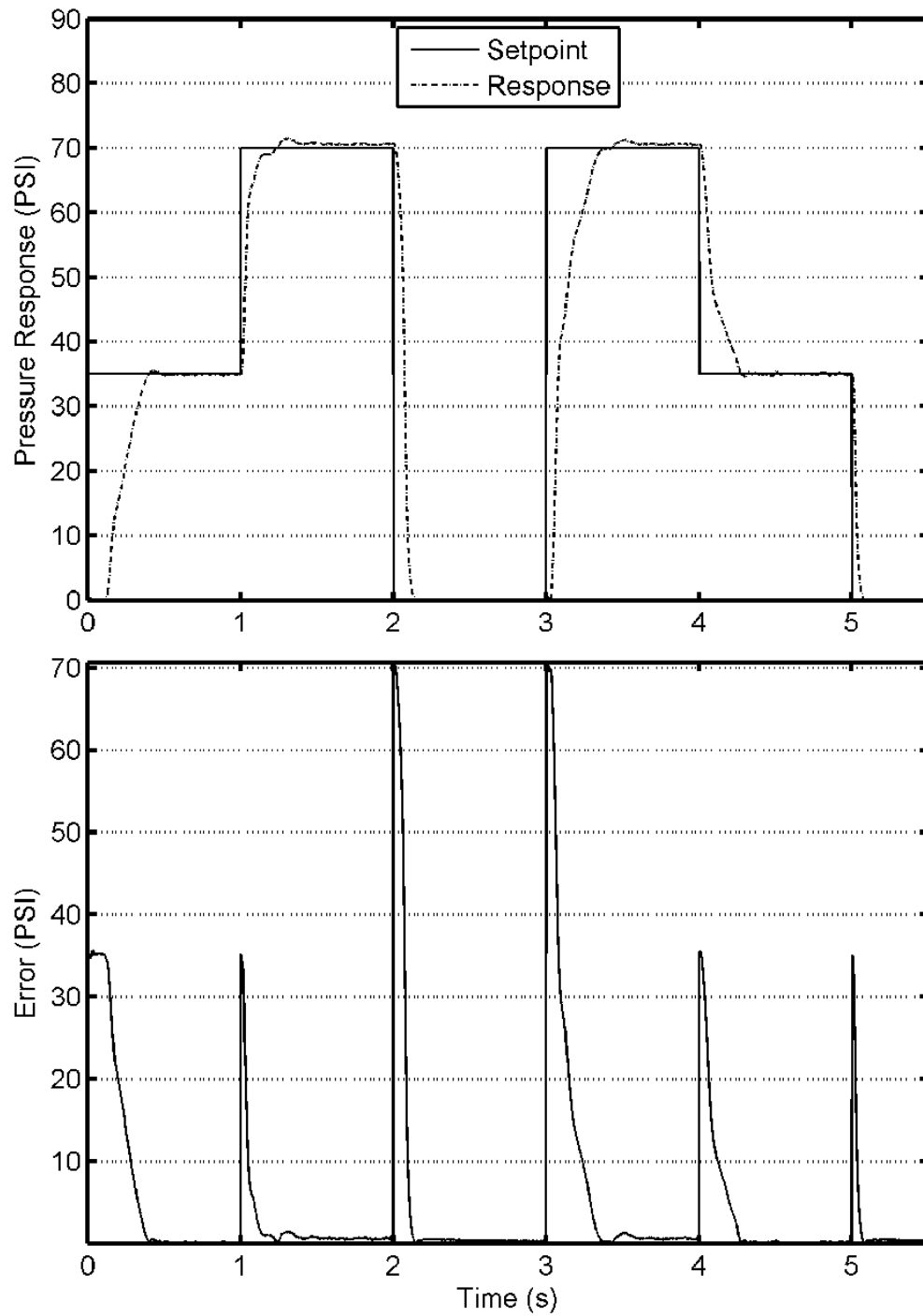


Figure 5.7 PID+ENFF controller pressure response and error for a multi-step setpoint.

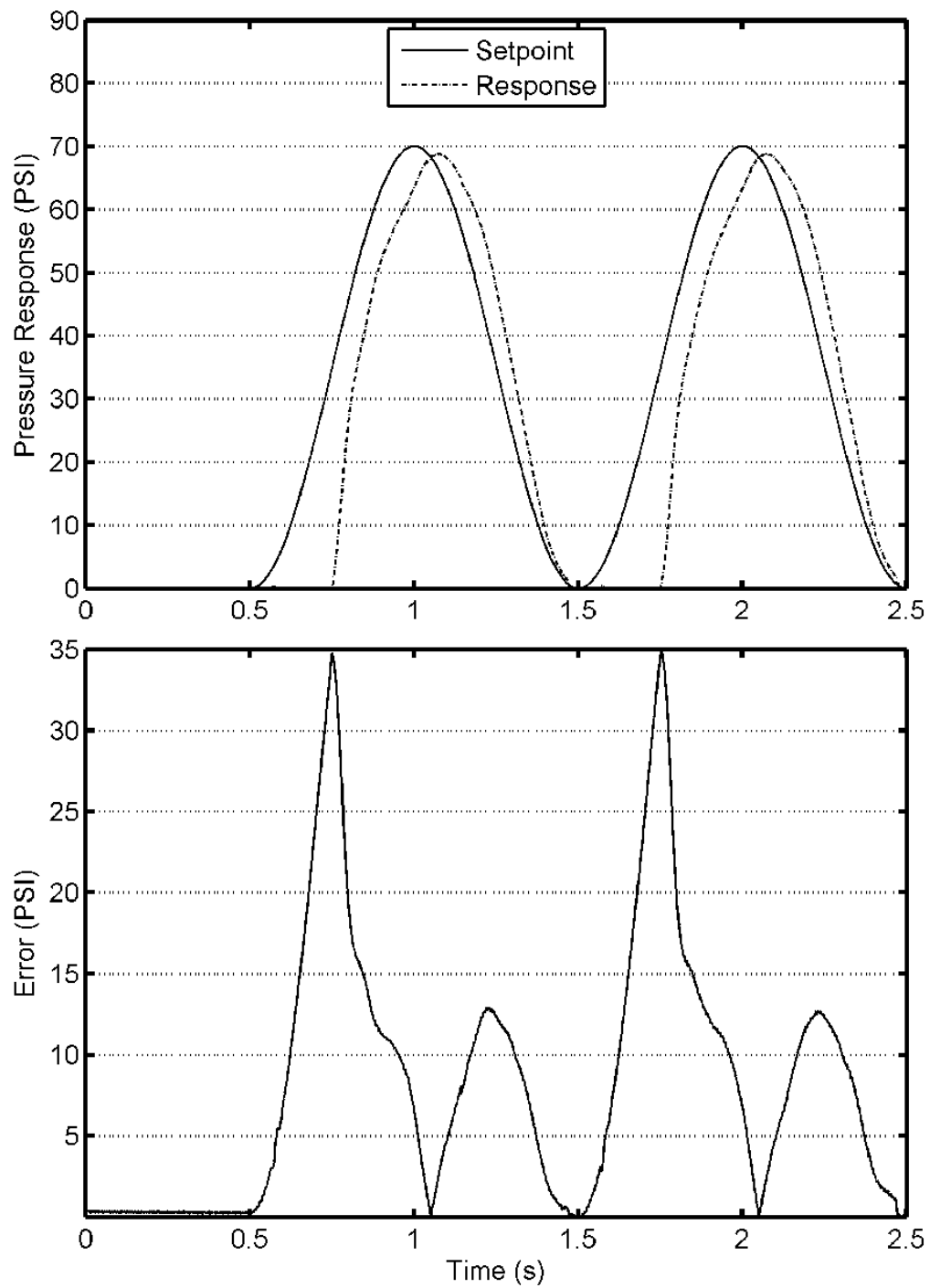


Figure 5.8 PID+ENFF controller pressure response and error for a cosine setpoint.

## 5.4 SMOOTHING

### 5.4.1 *Introduction*

In this context, “smoothing” refers to limiting the 2<sup>nd</sup> time derivative of the setpoint. This is analogous to limiting the acceleration if the setpoint was the desired position. Specifically, the smoothed multi-step setpoint was calculated by low-pass filtering it using a zero-phase second-order low-pass filter with both discrete time poles at 0.9. It was expected that this smoothed setpoint would reduce the overshoot and pressure errors compared to a step change since it is less demanding on the controller.

### 5.4.1 *Results*

The pressure responses for unsmoothed and smoother 35 PSI step setpoints are shown in Figures 5.10 and 5.11, respectively. Their performance metrics are listed in Table 2. Using the smoothed step improved in the mean error by 21%, reduced the max. abs. error by 2 PSI and increased the response time by 33%. The increased response time is undesirable. However, if the pressure is meant to reach (within 2%) its setpoint by a specific time then the smoothed setpoint can simply be shifted earlier to correct for the longer response time. This was not done in the current implementation since it would have prevented fair comparisons with the other tests.

While this smoothing reduced overshoot in some cases, it did not help to reduce the large overshoot the system experiences when the valve first opens. It was determined that the initial overshoot was caused by a combination of inertance of the water in the hoses, valve stiction and integral windup. The mitigation of the valve stiction and integral windup will be discussed in sections 5.6 and 5.7, respectively.

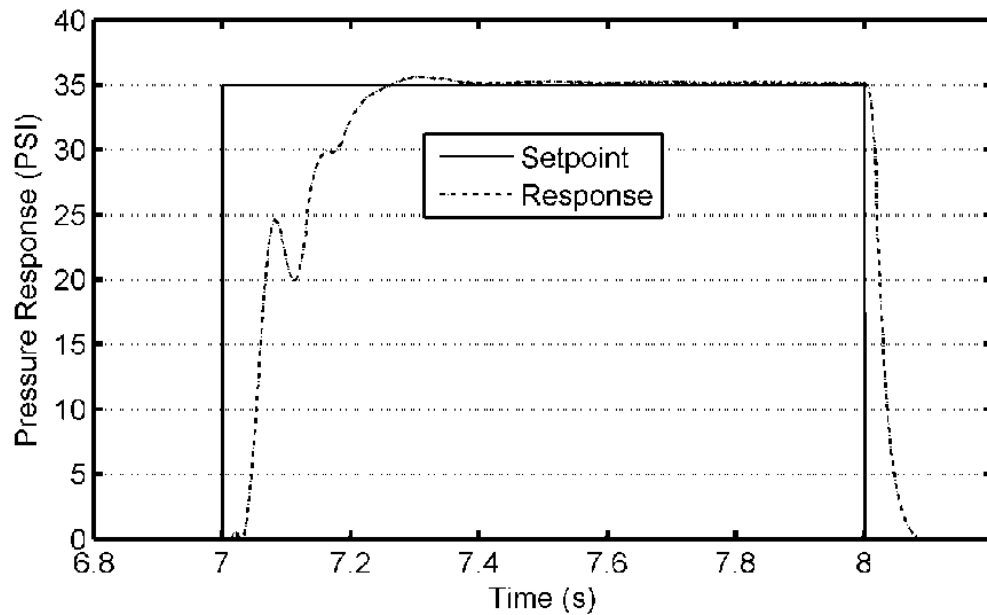


*Figure 5.9 PID+ENFF controller pressure response for an unsmoothed 35 PSI step setpoint.*

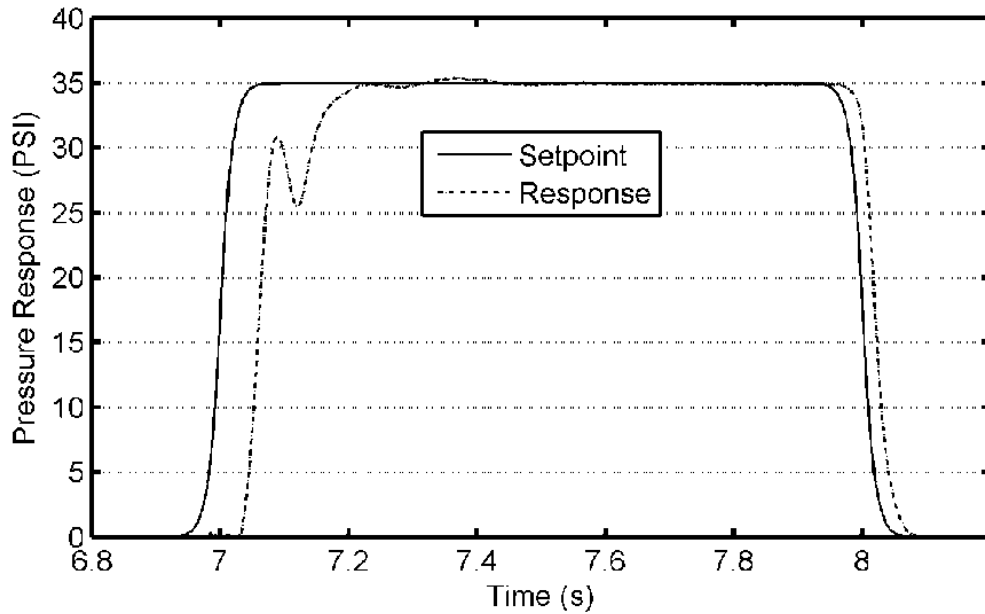


Figure 5.10 PID+ENFF controller for the smoothed version of the step setpoint from Figure 5.10.

Table 2 Comparison of PID controller performances for unsmoothed and smoothed 35 PSI step setpoints.

	Mean error (PSI)	Max. error (PSI)	Settling time for $\pm 2\%$ error (ms)
<b>Unsmoothed</b>	3.23	35	302
<b>Smoothed</b>	2.53	33	402

## 5.5 INTERACTION PROBLEM AND ITS SOLUTION

### 5.5.1 *Introduction*

The plant has three inputs of  $U_1$ - $U_3$ , and three outputs of  $P_1$ - $P_3$ , so it is a multiple input, multiple output (MIMO) system. This section explains the interactions between the different subsystems, and how this MIMO system is able to be considered as three single input single output (SISO).

### 5.5.2 *Interaction Problem*

The plant is a coupled MIMO system. This means that every input can influence every output in the system. The reason is the three subsystems are supplied by single pump and manifold. If any valve opens the other valves experience a drop in pressure and flow rate as the water is 'split'. As the nozzles can be approximated by hydraulic resistors, this splitting is explained by Kirchoff's current law.

When a single valve is open the ENFF equation applies to that particular subsystem and the system will operate as intended. The problem is, since the plant includes multiple valves, as each valve opens the manifold pressure will drop, affecting all of the subsystems. The cause of the pressure drop is that the pump's flow capacity is nearly capped. When a pump is running at maximum flow rate the pressure supplied is

zero. This is illustrated by the pump curve in Figure 5.11. When all three valves are fully open this pump is operating near it max flow rate and the pressure drops significantly.

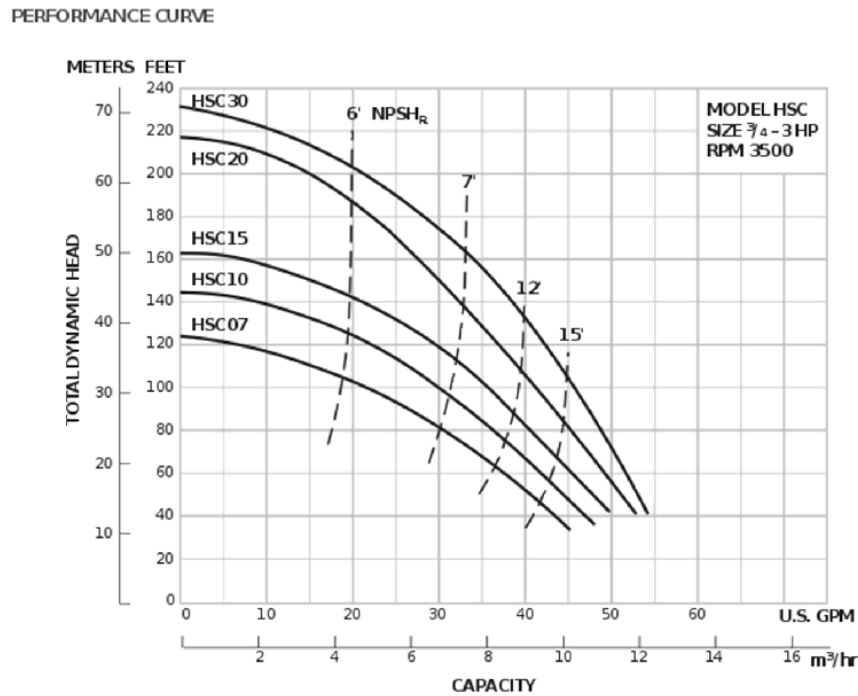


Figure 5.11 Pump curve for the HSC-20 pump used in the apparatus.

An example of the problem is shown in Figures 5.13-5.14. The pressure setpoint for the 1st subsystem held at 35 PSI. Its error increases dramatically when valve 2 is opened. Examining the response of pressure 2, it does not reach its pressure setpoint due to valve 1 being open. The

errors are very slowly decreasing due to an inadequate integral component in the PID+ENFF controller.

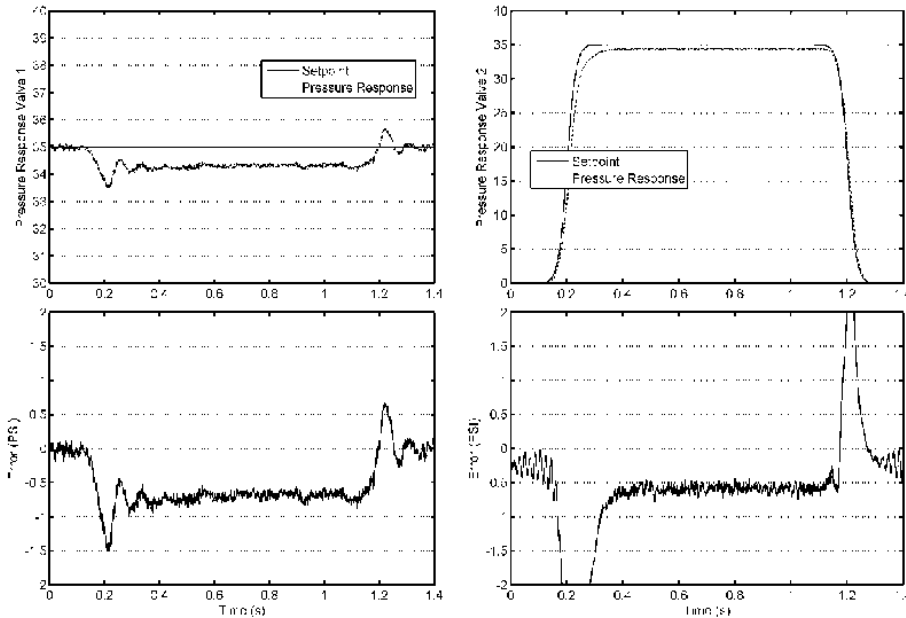


Figure 5.12 and Figure 5.13 Left: Pressure setpoint, response and error for 1<sup>st</sup> subsystem. Right: Pressure setpoint, response and error for 2<sup>nd</sup> subsystem.

### 5.5.3 Solution

The solution to this problem was found to be increasing the integral gain for each subsystem by about 50%. This solution is simple, but problematic. Increasing the integral gains corrected the errors caused by another valve opening, but also caused large oscillations whenever a setpoint change occurred. This was expected because it is known that increasing the integral gain will typically increase the size of the

overshoot. Figure 5.13 shows the results produced using the higher integral gains. The steady state pressure errors are much better than in Figure 5.12, at the expense of introducing large oscillations. In particular pressure 1 has an overshoot of 9 PSI or 25% which is unacceptable. The large oscillations also produce loud noises that are disturbing to the operator. This secondary problem was solved by limiting the size of the integral component as discussed in section 5.7.

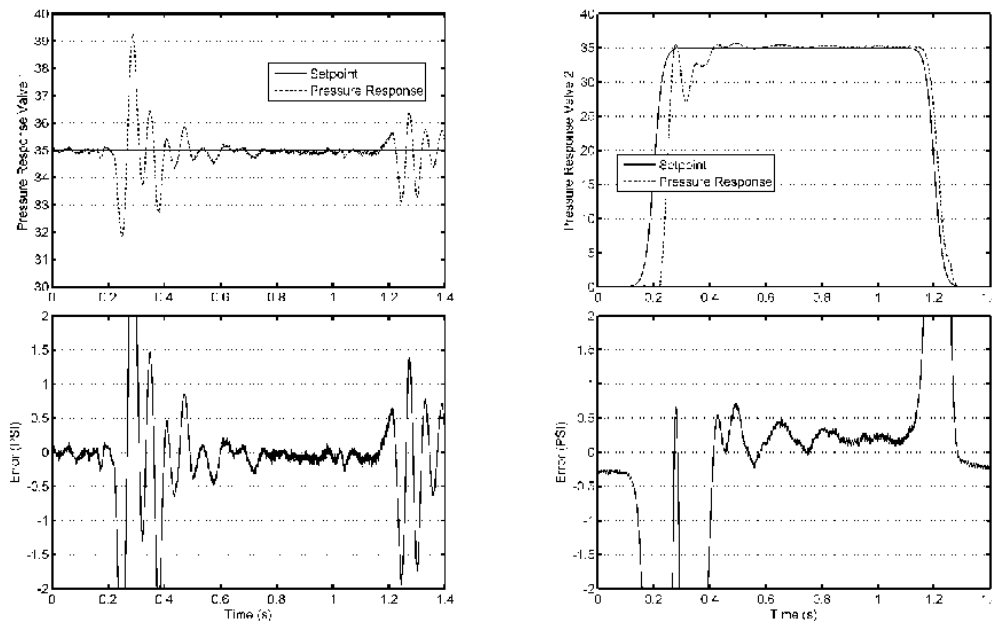


Figure 5.14 Results produced for subsystems 1 and 2 using higher integral gains.

## 5.6 MITIGATION OF VALVE STICTION

With this plant, valve stiction is rare but still causes significant problems. Due to the design of the valve, stiction only occurs when the valve is first opened. In other words, the valve needs to be shut fully before stiction will occur. This valve stiction reduces the effectiveness of the integral term's ability to compensate for the interaction error. Additionally this stiction was observed to destabilize the controller during the first seconds in some of the experiments. It was discovered that if the valve was open before running the controller the system worked well. This observation led to the creation of two biases that were incorporated into the controller.

The valve is most stuck when it is opened at the beginning of a run. The obvious way to fix this was to add a 'kick' when the system is first started. This was done by adding a 10 PSI bias to the setpoint at timestep zero. This causes the controller to generate a voltage spike. This spike charges the solenoid coils, generating the forces required to overcome the stiction.

After the first timestep the pressure bias is reduced to 2 PSI. This value was empirically determined. This 2<sup>nd</sup> bias prevents the valve from ever fully closing thereby mitigating stiction. Additionally it keeps the hoses primed; this keeps water in the line, eliminating air bubbles and shortening the time it takes for the nozzle to develop a proper spray pattern. Note that the 2<sup>nd</sup> bias is insufficient to spray water out of the nozzle, so the water only drips. Since the nozzles are placed below the mould this is not a problem. Finally, after the program finishes, the controller send a zero voltage value to the valve for 100 ms before shutting down. This is required as it takes time for the valves to correctly seal. Failure to do so would result in continuous leakage, wasting water.

## 5.7 WINDUP PREVENTION USING INTEGRAL BOUNDING

### 5.7.1 *Introduction*

During testing it was apparent that even with the inclusion of the ENFF component, considerable integral effort is required because of the multiple valves and the varying pressures, as discussed in sections 5.5.2 and 5.5.3. This led to the problem of integrator windup (Bucella 1997).

### 5.7.2 Solution

The windup problem was solved by simply bounding the numerical integration in (5-5) as follows:

$$U(t_k) = f(P_{des,j}(t)) + K_{P,j}e_j(t_k) + K_{I,j}sat\left(\sum_{i=0}^k (e_j(t_i))T\right) + K_{d,j}\frac{e_j(t_k) - e_j(t_{k-1})}{T}$$

5-6

where

$$sat(x) = \begin{cases} I_{bound} & \text{if } x > I_{bound} \\ -I_{bound} & \text{if } x < -I_{bound} \\ x & \text{otherwise} \end{cases}$$

and  $I_{bound}$  is the manually tuned bound. The corresponding block diagram is shown in Figure 5.14. This simple change allowed a large integral gain to be used without the integral component of  $U_j(t_k)$  becoming excessively large.

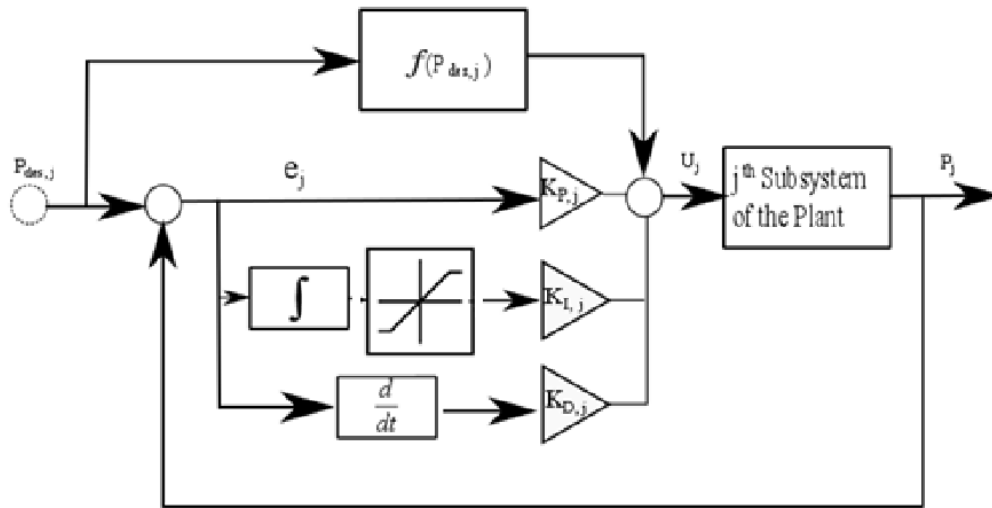


Figure 5.15 Block diagram of the PID+ENFF controller with integral bounding for one subsystem of the plant.

### 5.7.3 Results

Results obtained without and with integral bounding for a smoothed 35 PSI setpoint are shown in Figures 5.15 and 5.16, respectively. These results show that integral bounding can greatly reduce the overshoot caused by the integral component of the valve control voltage.

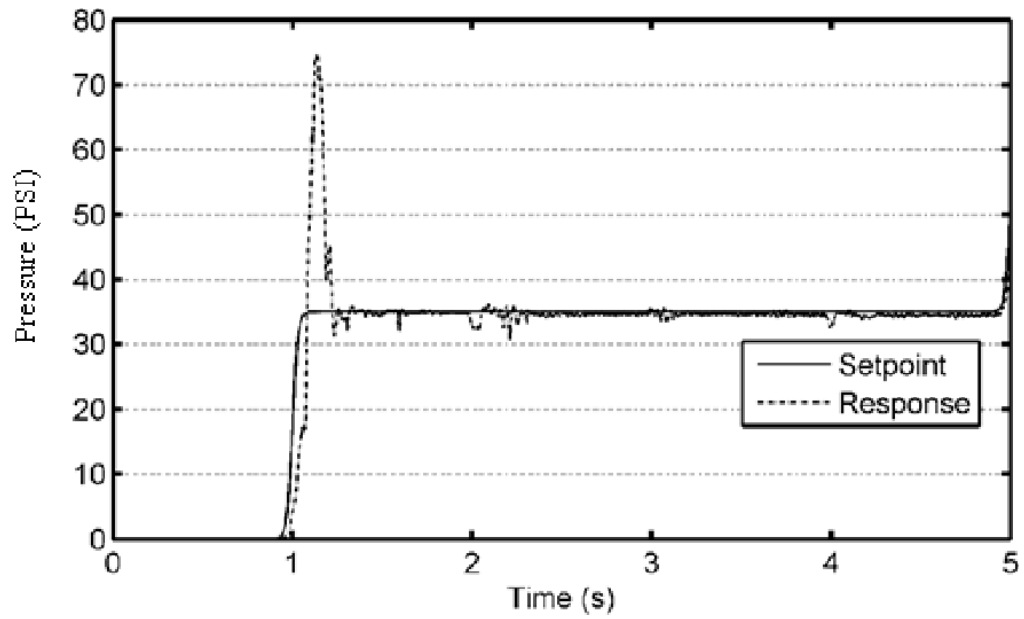


Figure 5.16 Pressure response for PID+ENFF controller without integral bounding.

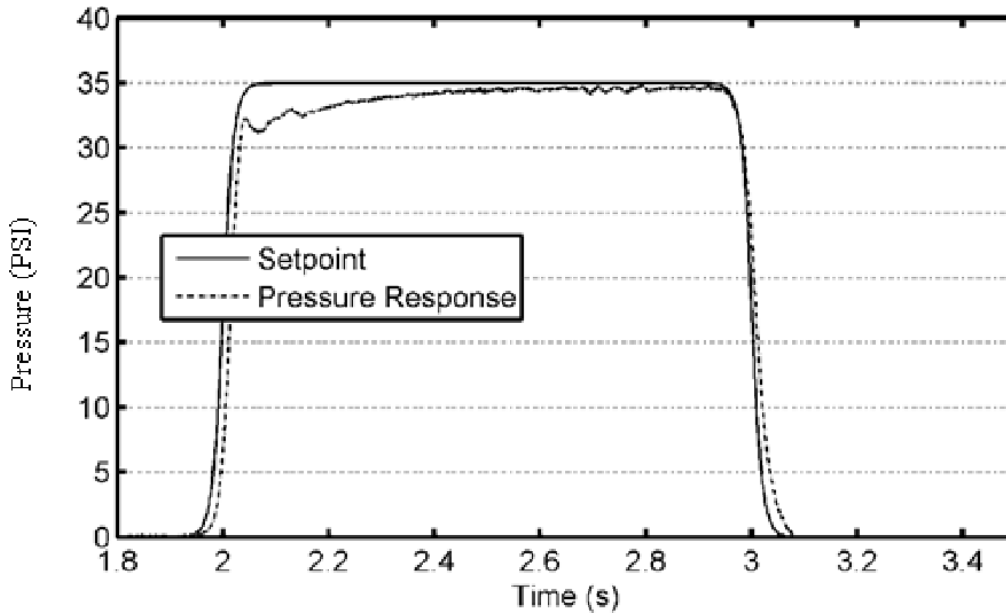


Figure 5.17 Response for PID+ENFF controller after integral bounding.

## 5.8 ALTERNATIVE PID

### 5.8.1 *Introduction*

An alternative PID (APID) controller was developed that uses the ENFF equation in a different way. Several versions were attempted, and the only one that worked was putting the sum of a PID output plus the setpoint into the ENFF equation. Its block diagram is shown in Figure 5.20. Its discrete time equation is:

$$U(t_k) = f \left( \left( P_{des,j}(t) \right) + K_{P,j} e_j(t_k) + K_{I,j} \text{sat} \left( \sum_{i=0}^k (e_j(t_i)) T \right) \dots \right. \\ \left. + K_{D,j} \frac{e_j(t_k) - e_j(t_{k-1})}{T} \right)$$

(5-7)

The PID gains were manually tuned.

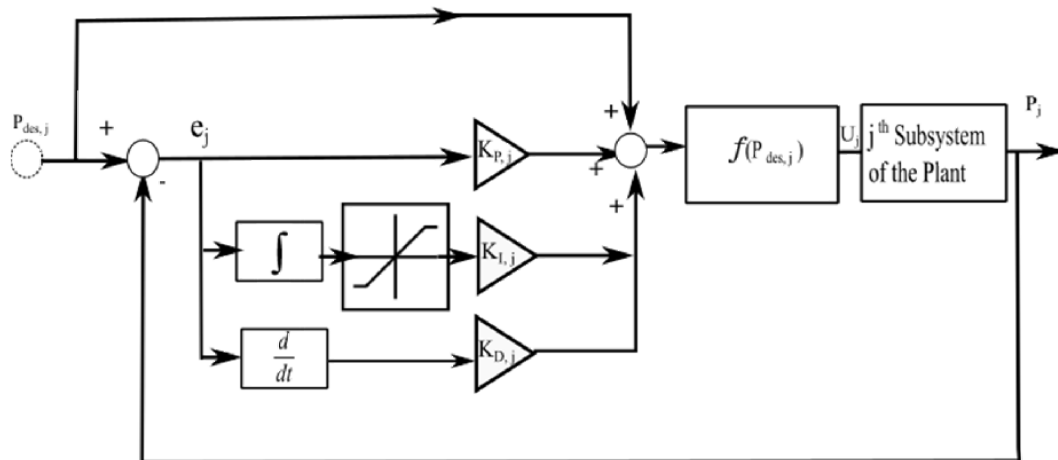


Figure 5.18 APID controller block diagram for one subsystem of the plant.

### 5.8.2 *Preliminary Results*

Results for the APID controller with multi-step and cosine setpoints are shown in Figures 5.18 and 5.19, respectively. Very little time was available to tune the gains so these results are very preliminary. The results for the multi-step setpoint are quite good for the first 4 s, but some large oscillations then appear when the pressure is stepped down from 80 to 35 PSI. It is likely that this was caused by the ENFF equation since it was only intended to account for quasi-static behavior whereas the sudden changes in this setpoint are very dynamic. The results for the cosine setpoint are more encouraging, however the tendency of this APID controller to oscillate is still apparent in the error plot in Figure 5.19.

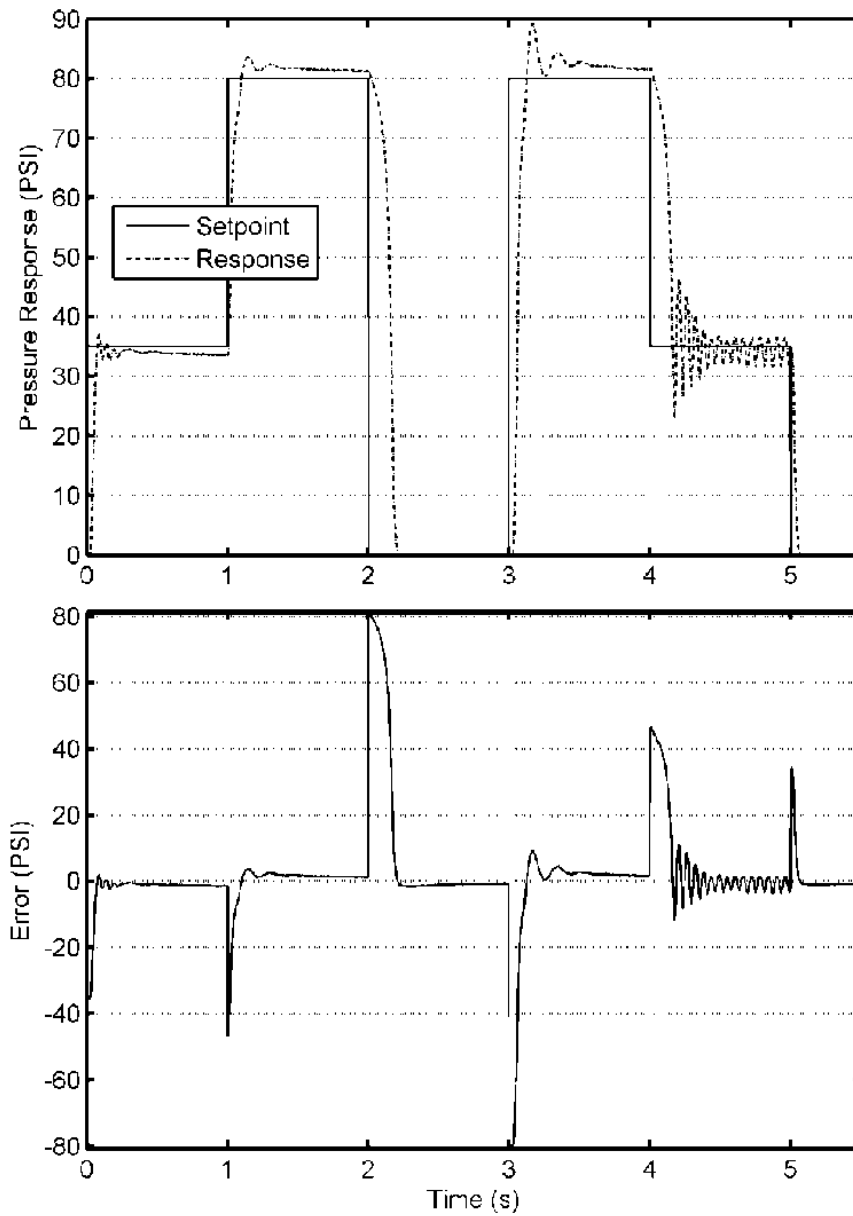


Figure 5.19 APID controller pressure response and error for a multi-step setpoint.

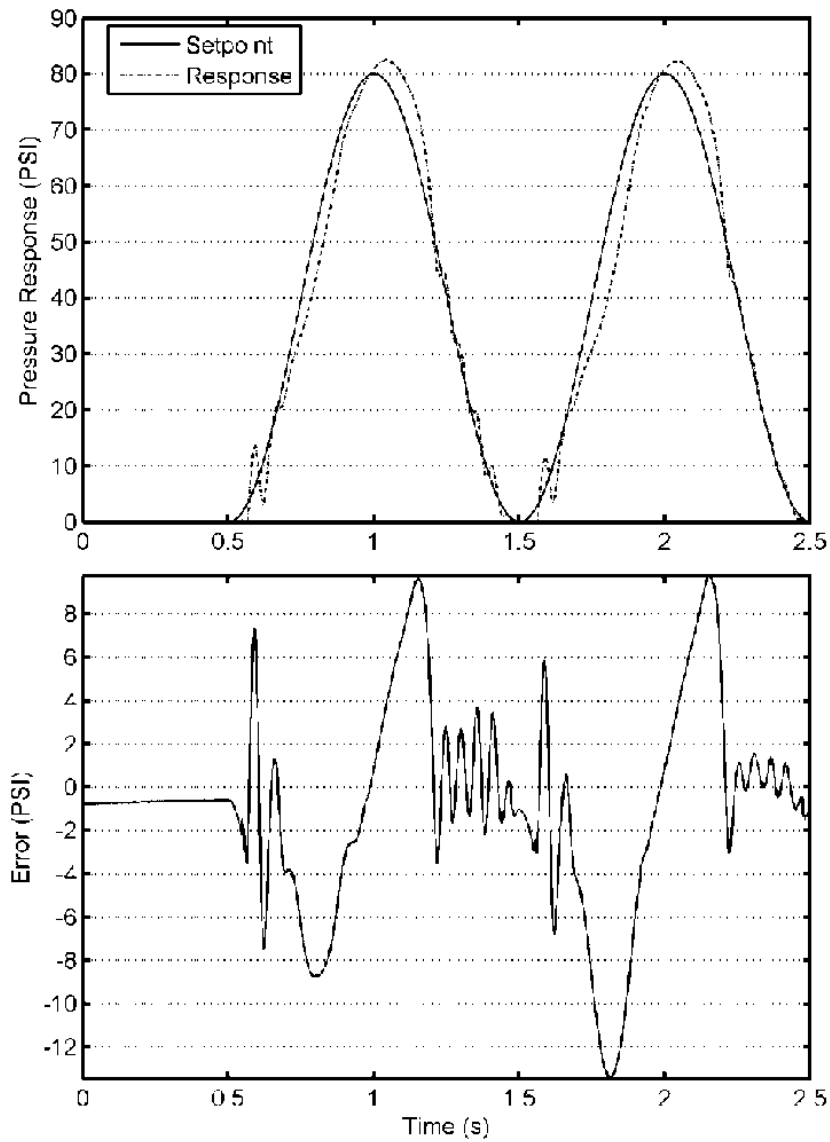


Figure 5.20 APID controller pressure response and error for a cosine setpoint.

## 5.9 EXTENDED PID CONTROLLER

### 5.9.1 *Introduction*

The final version of the controller included the PID plus the several extensions that were developed, and was termed the Extended PID (EPID) controller. The extensions consist of the ENFF component, setpoint smoothing filter, pressure biasing and integral bounding presented in sections 5.3-5.8. The block diagram of the EPID controller is presented in Figure 5.21.

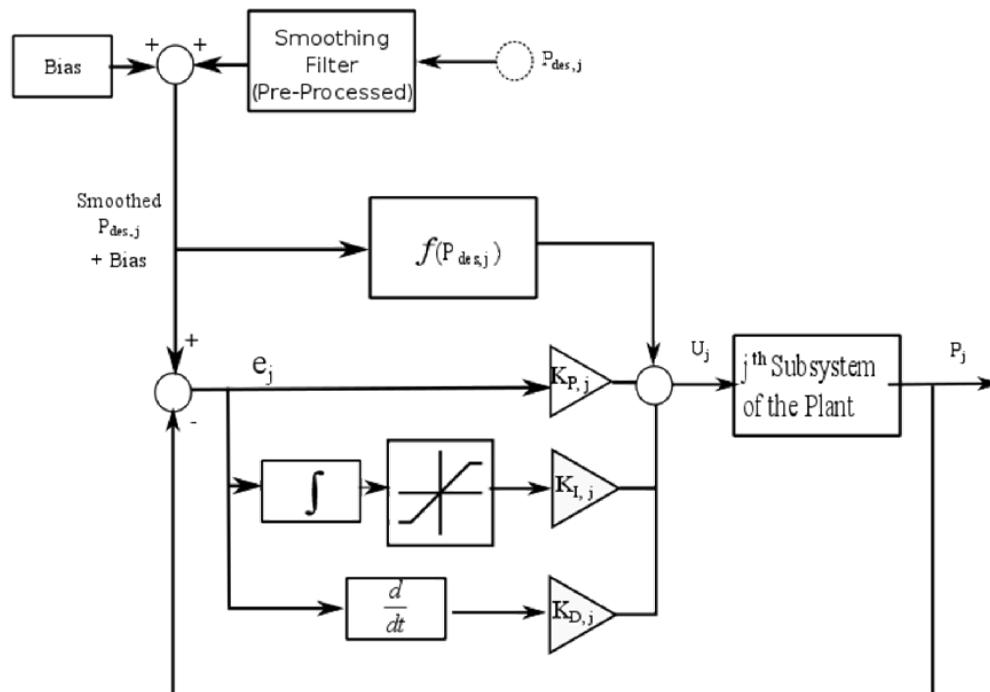


Figure 5.21 EPID controller block diagram for one subsystem of the plant.

### 5.9.2 *Results*

Example multi-step and cosine setpoint results for the EPID controller are shown in Figures 5.21 and 5.22, respectively. Compared with the PID+ENFF results, the response for the multi-step setpoint is much faster. The improvements with the cosine setpoint are even more noticeable. Comparing Figures 5.8 and 5.22 the EPID has dramatically reduced the error and lag between the setpoint and response. The max. abs. error was reduced from 33 PSI to only 3.2 PSI. A detailed quantitative comparison of the controllers performances is presented in the next section.

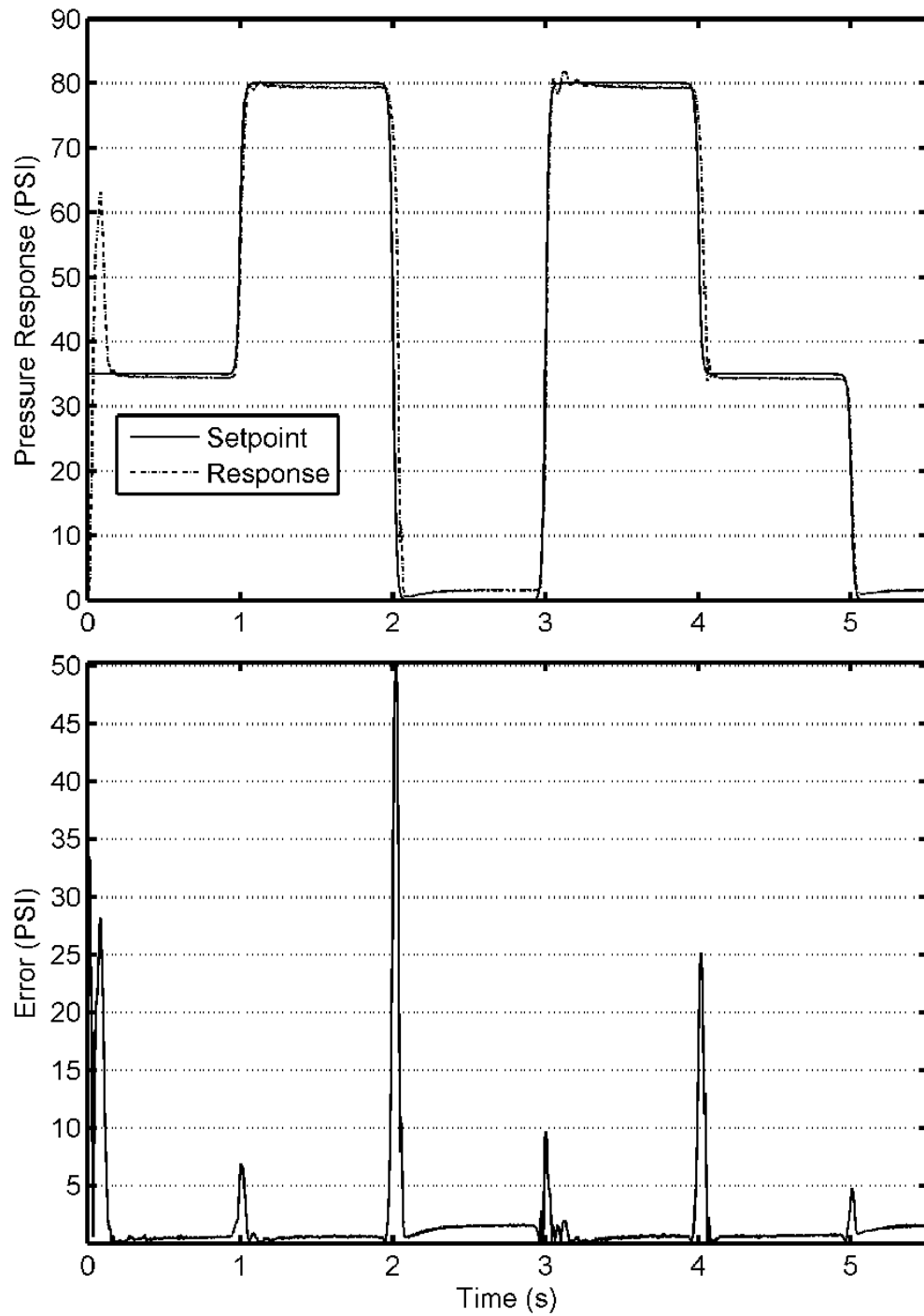


Figure 5.22 EPID controller pressure response and error for the multi-step setpoint.

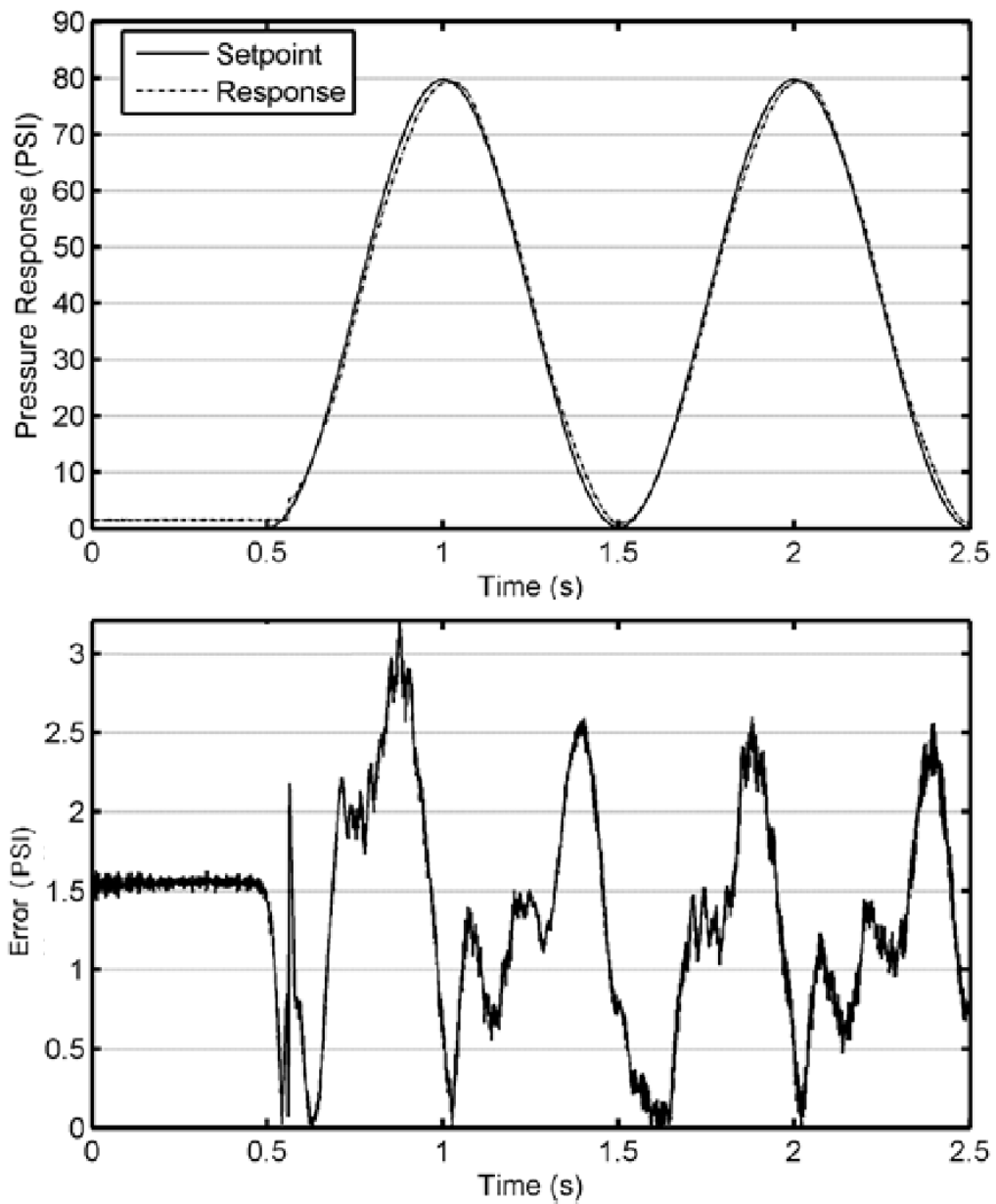


Figure 5.23 EPID controller pressure response and error for the cosine setpoint.

### 5.10 DETAILED QUANTITATIVE COMPARISON

Mean error, mean abs. error and max. abs. error performance metrics for the four controllers are tabulated in Tables 3-6. These results were averaged from five tests conducted using each controller. Additional plots are presented in Appendix B, and the performance metrics from all tests are tabulated in Appendix C. Every controller except the APID was very repeatable with standard deviations of mean error, mean abs. error and max. abs. error all less than 0.2 PSI (for the standard deviations see the 12 tables in Appendix C). The APID experienced some unusual behaviors during the step tests as discussed in section 5.8.2. In the remainder of this section the results in Tables 3-6 will be compared.

The standard PID controller had the worst performance as expected. The addition of the ENFF component provided significant improvements, particularly to the mean abs. error and max. abs. error. The mean abs. error was reduced by 36% averaged over the four setpoints, while the max. abs. error was reduced by 26% on average. The EPID controller provided the best performance. It improved all metrics compared to the PID+ENFF. Averaged over the four setpoints, the mean abs. error and max. abs. error were reduced by 73% and 57%, respectively. Finally, the APID controller produced the 2<sup>nd</sup> best overall performance. It is

important to note that the 5<sup>th</sup> multi-step setpoint test (plotted in Figure 5.20) had periods of large oscillation which negatively influenced the averages presented in Table 6, causing them to be worse than the PID+ENFF results. The improvement relative to PID+ENFF can be observed in the results for the cosine and ramp setpoints. Averaged over those three setpoints, the mean abs. error and max. abs. error were reduced by 45% and 63%, respectively.

*Table 3 PID performance metrics.*

<b>Setpoint</b>	<b>Mean Error (PSI)</b>	<b>Mean Abs. Error (PSI)</b>	<b>Max. Abs. Error (PSI)</b>
Multistep	1.7	7.2	78.9
Cosine	3.8	11.7	56.1
Fast Ramp	2.1	6.8	31.7
Slow Ramp	0.5	1.6	13.7

*Table 4 PID+ENFF performance metrics.*

<b>Setpoint</b>	<b>Mean Error (PSI)</b>	<b>Mean Abs. Error (PSI)</b>	<b>Max. Abs. Error (PSI)</b>
Multistep	-1.50	5.3	70.7
Cosine	-3.5	8.2	35.0
Fast Ramp	-1.4	3.4	20.0
Slow Ramp	-0.2	0.5	7.0

*Table 5 EPID performance metrics.*

<b>Setpoint</b>	<b>Mean Error (PSI)</b>	<b>Mean Abs. Error (PSI)</b>	<b>Max. Abs. Error (PSI)</b>
Multistep	0.7	1.9	50.3
Cosine	0.4	1.4	3.2
Fast Ramp	0.1	0.8	2.1
Slow Ramp	-0.1	0.6	1.6

*Table 6 APID performance metrics.*

<b>Setpoint</b>	<b>Mean Error (PSI)</b>	<b>Mean Abs. Error (PSI)</b>	<b>Max. Abs. Error (PSI)</b>
Multistep	2	6.5	81.3
Cosine	-0.8	3.3	9.8
Fast Ramp	-1.1	2.1	7.5
Slow Ramp	-0.9	1.3	5.7

### 5.11 CONCLUSION

After determining that a standard PID performed poorly, the ENFF component was created by fitting an inverse model to experimental data. The combined PID+ENFF controller was further extended based on knowledge of the plant and experimentation to create the EPID controller. A preliminary investigation of the APID controller suggested it is worthy of future study. The EPID controller produced the best performance of

the four controllers. It has a very fast response and can precisely track multi-step, cosine and ramp pressure setpoints; as shown by the plots and tabulated results. Averaged over five experiments, its mean error was 0.9% (0.7 PSI) for a multi-step setpoint which is well within the 2% limit established for this project. It produced even smaller mean error values for the cosine, fast ramp and slow ramp setpoints.

## ***CHAPTER 6. CONCLUSION***

### ***6.1 SUMMARY AND ACHIEVEMENTS***

This thesis presented a novel solution for controlling an economical, low pressure, high speed and high flow rate hydraulic spraying apparatus. After studying the material properties and the requirements of the casting process, an apparatus was developed to support and contain the array of sprayers. This hydraulic system's plant experienced considerable hysteresis and highly nonlinear open-loop dynamics. These dynamics are problematic to linear controllers such as a PID. Within this thesis, four controllers were experimentally investigated as follows: standard PID (as a baseline), PID plus empirical nonlinear feedforward (PID+ENFF), an extended PID (EPID) and an alternative version of PID (APID).

For a cosine setpoint, the PID produced a mean abs. error of 13%, max. abs. error of 70% and mean error of 4%. For a multi-step setpoint, these values were 9%, 91% and 2% respectively. With the PID+ENFF the performance improved significantly. In particular, for a 35 PSI step the PID+ENFF reduced the overshoot from 43% to almost zero. For the cosine setpoint, the PID+ENFF produced a mean abs. error of 10%, max. abs. error of 43% and mean error of 1.8%. While the PID+ENFF met the 2%

mean error requirement, its response was still quite slow and its gains were very difficult to tune. The controller was further extended in an effort to improve its performance. The first extension was smoothing the setpoint. Limiting the rate of change of the setpoint helped to reduce the error while slightly increasing the response time. Next, the integrator was bounded. This greatly reduced the overshoot caused by integral windup. A bias was added to the setpoint at time zero to overcome the starting stiction. Additionally, a smaller bias was added to all afterwards, to prevent the valve from ever fully closing. By slightly opening the valve, stiction was reduced, and the hoses were primed. Priming the hoses maintained a small water pressure in the lines, removing air bubbles and almost eliminated the effects of water inrush. This extended PID (EPID) controller produced a 2.3% mean abs. error, a 4% max. abs. error and a 0.6% mean error for the cosine setpoint. For the multi-step setpoint, these values were 2.4%, 41% and 0.09%, respectively. Its performance was also highly repeatable. This EPID controller met all of the sprayer control requirements for this casting process, even with this difficult to control plant. The fourth controller was an alternate nonlinear version of PID control. The output of the PID was passed through the ENFF equations to obtain the valve control voltage. This provided the 2<sup>nd</sup> best performance

of the four controllers implemented, based on the preliminary investigation that was performed.

In addition:

The EPID controller is computationally light, allowing it to run quickly (i.e., 1 ms sampling period) on a standard PC. This would also allow the controller to run on less expensive equipment, such as the PLCs, FPGAs or microcontrollers used in industry.

This thesis provided insights as to how low pressure, high speed, high flow rate hydraulic systems operate. The research findings are potentially applicable to other quenching systems, agricultural spraying, water-based hydraulics and high speed flow control.

Altering the layout from one hose per valve; to two hoses per valve was very important. This subtle design change solved months of frustration by reducing the valves' nonlinearity and making tuning the controller achievable.

## **6.2 FUTURE WORK**

It is recommended that the current nozzles be replaced with more linear spraying nozzles. The nozzles used in this project do not have

linear flowrate/pressure responses, and using more linear nozzles will make the controller development and tuning easier. A linear nozzle may even make the ENFF component unnecessary. Additionally larger nozzles are easier to control, as are smaller valves. If the system is to be expanded to include more nozzles, a better hydraulic design should also reduce the complexity of the control problem.

Using pilot operated valves, as opposed to the direct-acting solenoid valves used in this research, should be investigated. A pilot operated valve should be less affected by the upstream and downstream pressures which would make the system easier to control.

Regarding the movable nozzles suggested in section 3.1, it is recommended that the motion is provided using hydraulic or pneumatic actuators. Only hydraulics (or pneumatics) can provide the force and environmental resistance required. The combination of caustic compounds, sand and hot water would destroy most electric actuation methods. The only ways electric actuators could be used is through elaborate force transmissions allowing them to be placed far away from the casting process (requiring more space than is currently available); or via environmental shielding which would too costly.

Due to the highly experimental nature of this project this apparatus is very versatile. However this versatility comes at a cost, because this device is so adaptable it is inferior at specific tasks. Due to the nature of research this project was in constant flux making it difficult to optimize the system. More materials information and having all the parameters 'set in stone' will greatly assist develop in the future.

Somewhat paradoxically, to the previous suggestion, allowing the controls engineer the ability to modify the part's design could facilitate better control of the process. This could not be done in this project due to the extremely tight geometry requirements.

**REFERENCE**

Bhadeshia, H. K. D. H. 1997. "Dendritic Solidification." *University of Cambridge / H. K. D. H. Bhadeshia.*

<http://www.msm.cam.ac.uk/phase-trans/dendrites.html>.

Bucella, Tim. 1997. *Servo Control of a DC-Brush Motor*. Teknic, Inc.

Caltech, Kenneth G. Libbrecht ~. 1999. *Snow Crystals.com*. Accessed July 2015.

<http://www.its.caltech.edu/~atomic/snowcrystals/primer/primer.htm>.

Chua, Gary W Crutz and Patrick S K. 2004. "Water Hydraulics Theory and Applications." *Workshop on Water hydraulics* 1-33.

David Weiss et al, John Grassi, Ben Shultz, and Pradeep Rohatgi. 2011.

"Testing the Limits of Ablation." *Modern casting* 26-29.

Dursun, Aykut. n.d. "Experimental Investigation Of The Sand Removal In Water-Soluble Sand Moulds Using Waterjets."

E. Doege\*, K. Droder. 2001. "Sheet metal forming of magnesium wrought alloys – formability." *Institute for Metal Forming and Metal Forming Machine Tools* 14-19.

Escolà, A. 2013. "Variable rate sprayer. Part 1 – Orchard prototype: Design, implementation and validation." *Computers and Electronics in Agriculture* 122-134.

Flemings, Merton C. 1974. *Solidification Processing*. McGraw Hill.

Harri Sairiala, Matti Linjama, Kari T. Koskinen and Matti Vileniu. 2002. "Proportional Velocity Control of a Water Hydraulic Cylinder Drive." *Fluid Power* 181-186.

I. Mudawar and WS.Valentine. 1989. "Determination of the Local Quench." *Journal of Heat Treatment* 107-121.

M.E.R Paice, P.C.H. Miller, W. Day. 1996. "Control requirements for spatially selective herbicide." *Computers and Electronics in Agriculture* 163-177.

Majed (Marv) Hamdan, Dr. Zhiqiang Gao. 2000. "A Novel PID Controller for Pneumatic Proportional Valves with Hysteresis." *IEEE* 1198-1201.

Minorsky, N. 1922. "Directional Stability of Automatically Steered Bodies."

*Journal of the American Society for Naval Engineers* 280 - 309.

Mudawar, T.A. Deiters and I. 1989. "Optimization of Spray Quenching

for." *Journal of Heat Treatment* 9-18.

Mudawar, W.S. Valentine and I. 1989. "Determination of the Local

Quench." *Journal of Heat Treatment* 107-121.

Nitin Karwa, Peter Stephan. 2012. "Jet Impingement Quenching: Effect of

Coolant Accumulation." *6th European Thermal Sciences Conference*.

IOP Publishing Ltd. 9.

Prescenzi, Anthony D. 2015. "Cast Body Nodes for 2016 Acura NSX." *SAE*

*International*.

Richard A. Hardin, Kai Liu, Atul Kapoor, And Christoph Beckermann.

2002. "A Transient Simulation And Dynamic Spray Cooling Control

Model For Continuous Steel Casting." *Metallurgical and Materials*

*Transactions*, September 17.

Shankar, Dr. Sumanth. 2013. "714 Solidification Notes and Classroom

Discussion." September -> December.

Takrouri, Kifah. 2015. "Personal Communication."

Tsuyoshi Yamada, Kazuhisa Ito. 2012. "Simple Adaptive Control of Water Hydraulic Servo Cylinder System." Chengdu, China: International Conference on Mechatronics and Automation, August 5 - 8.

United States Government, Environmental Protection Agency and the Department of Transportation of the United States of. 2010. "National Highway Traffic Safety Administration 40 CFR Parts 85, 86, and 600; 49 CFR Parts 531, 533, 536, et al. Light-Duty Vehicle Greenhouse Gas Emission Standards and Corporate Average Fuel Economy Standards; Final Rule." n/a: National archives and Records Administration, may 7.

**APPENDIX A: SETPOINTS USED IN THE**  
**EXPERIMENTS**

**A1: OVERVIEW**

The setpoints used to validate the controllers were: multi-step, cosine, a fast ramp and a slow ramp to represent a near quasi-static change. These were chosen to test a wide range of rates of change. The multi-step setpoints were of greatest interest, while the cosine and ramp functions were employed to ensure the system did not have some underlying flaw that was not revealed by the multi-step tests.

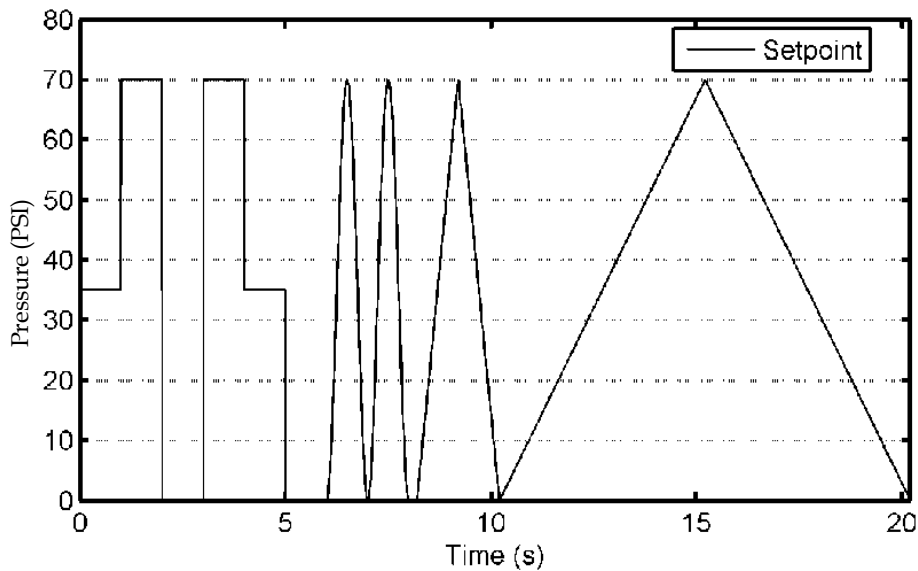


*Figure A1 : Setpoints used for each 20 second experiment.*

**A2 : MULTI-STEP SETPOINT**

This setpoint consists of steps from zero, to  $\frac{1}{2}$  max, to max, and back to zero with a one second hold on each step. These steps were then repeated in backwards order to provide more variation to the system.

**A3 : COSINE**

A cosine setpoint was selected to show how well the system responds to smooth transitions. It was simply a cosine wave changing from 0 to max to 0 over 1 second.

**A4 : FAST RAMP**

This setpoint consisted of a ramp from 0 to max over 1 second, then a ramp back down to 0. This shows the ability of the system to track a constantly moving setpoint with a constant rate of change.

**A5: SLOW RAMP.**

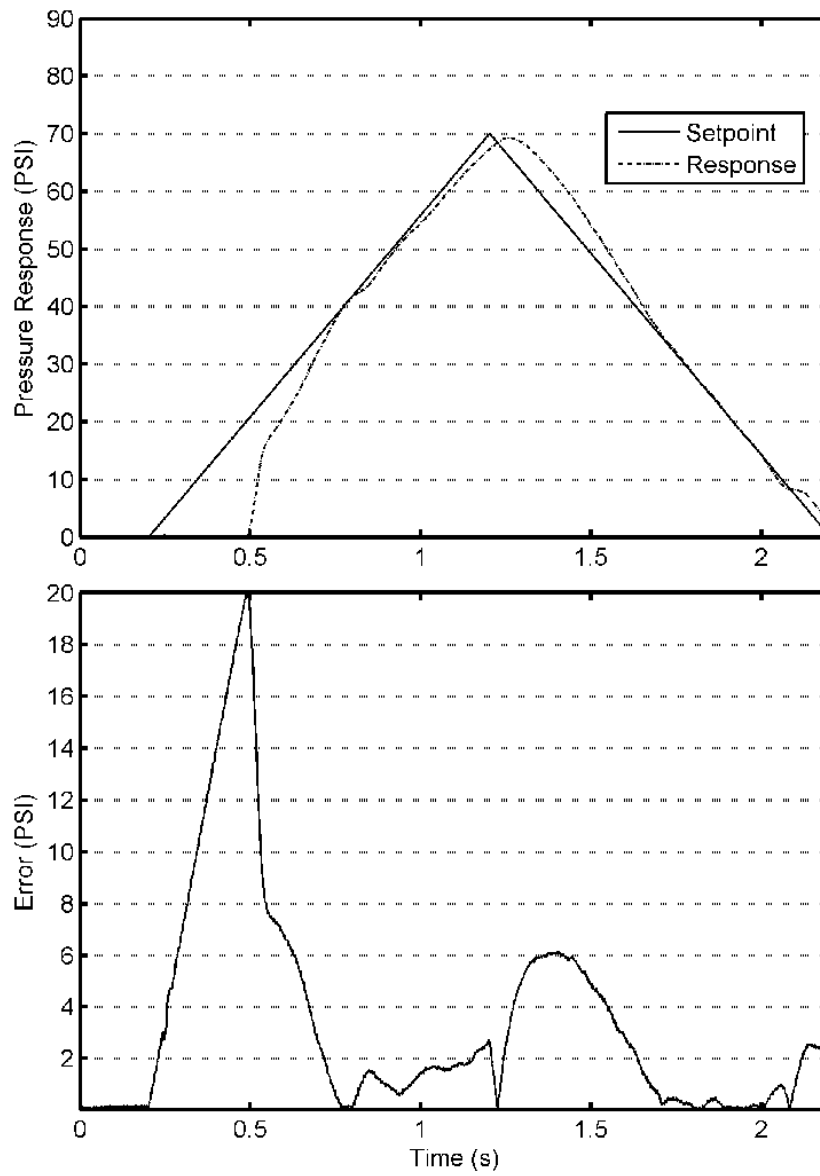
This slow ramp setpoint shows approximately how the system would perform at different static setpoints. It ramps from 0 to max over 5 seconds, then back down to 0.

**APPENDIX B: ADDITIONAL EXPERIMENTAL**

**RESULTS**

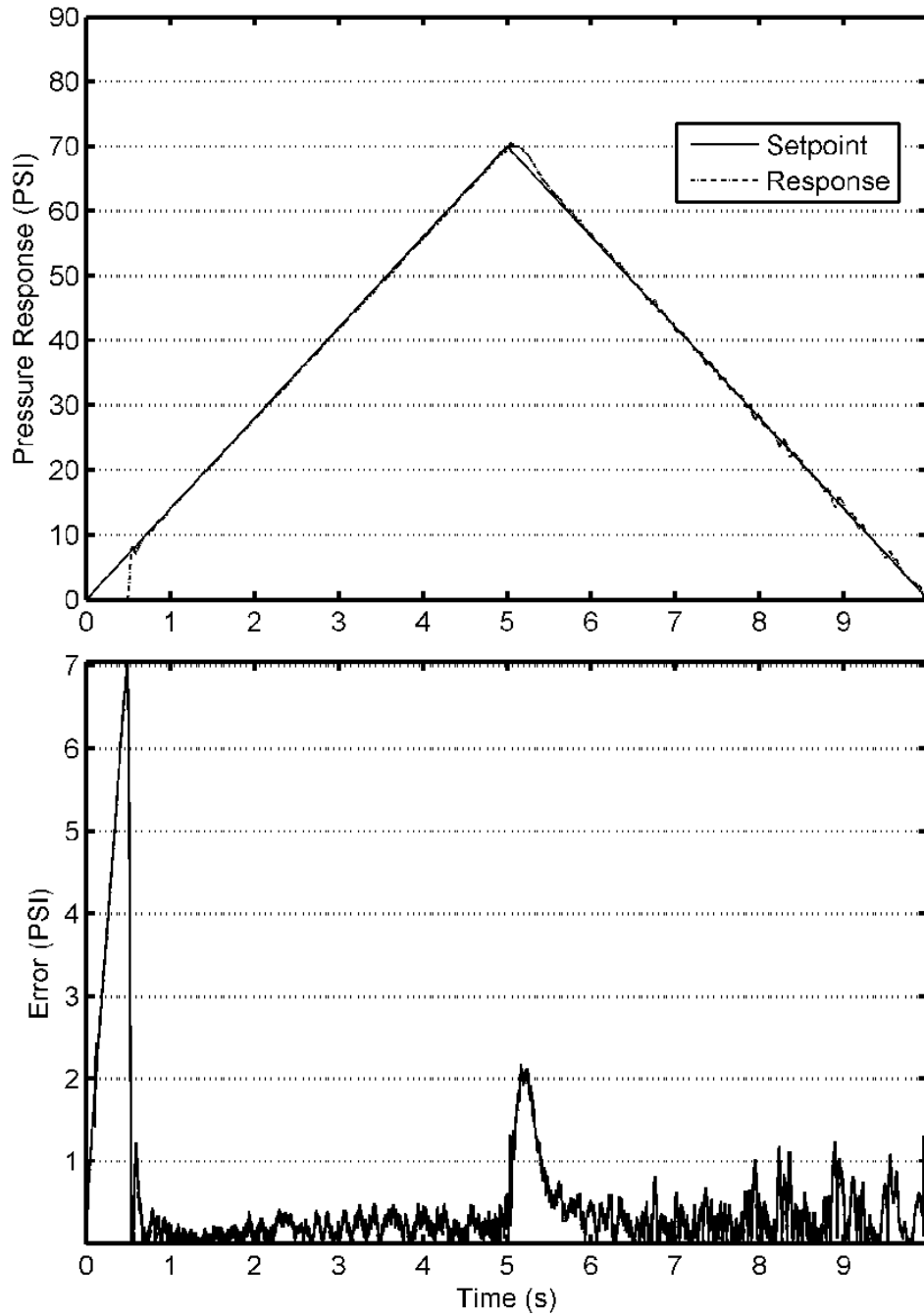
**B1: PID**

***B1.1 Fast Ramp***



*B.1 Fast ramp response for PID*

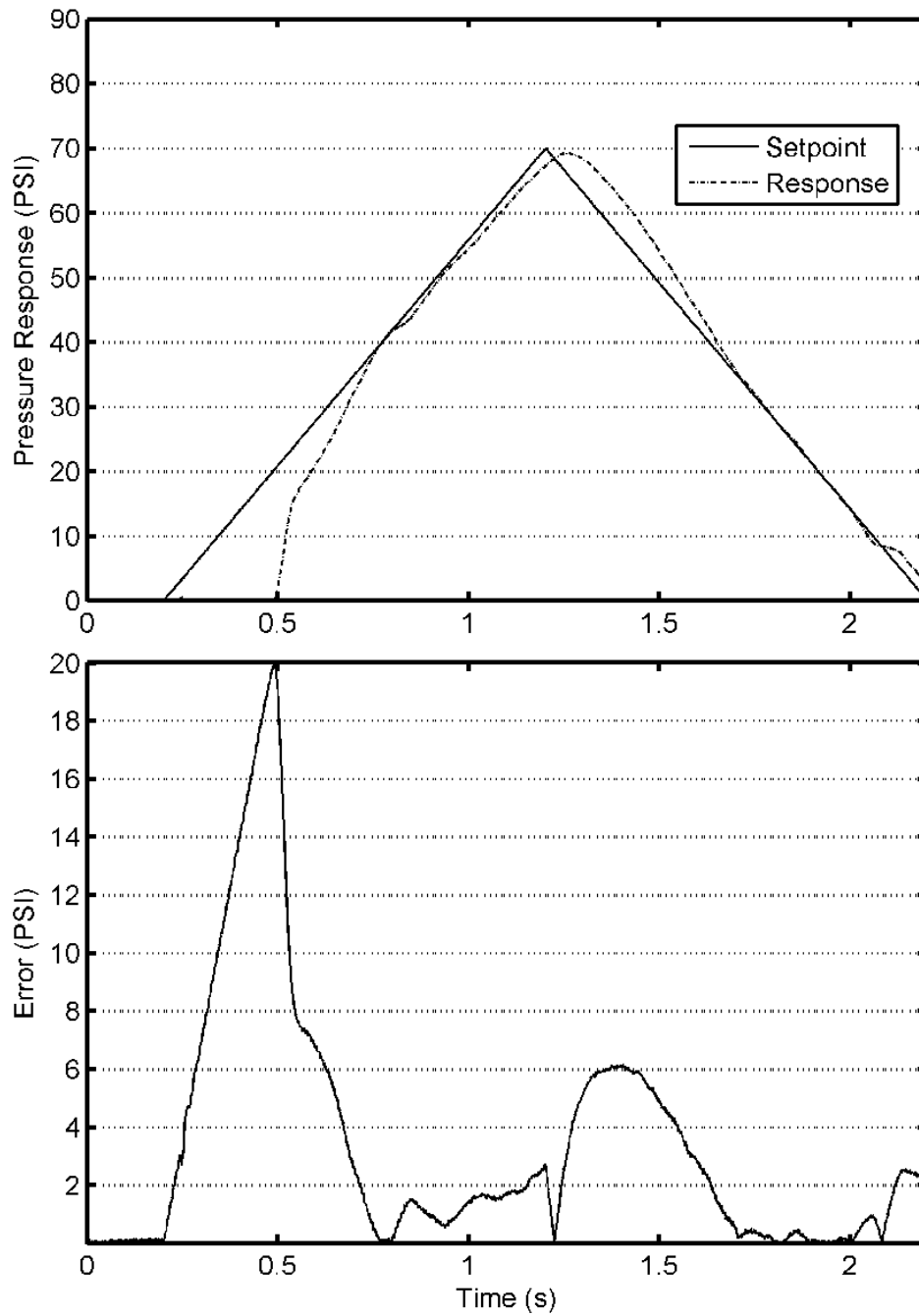
*B1.2 Slow ramp*



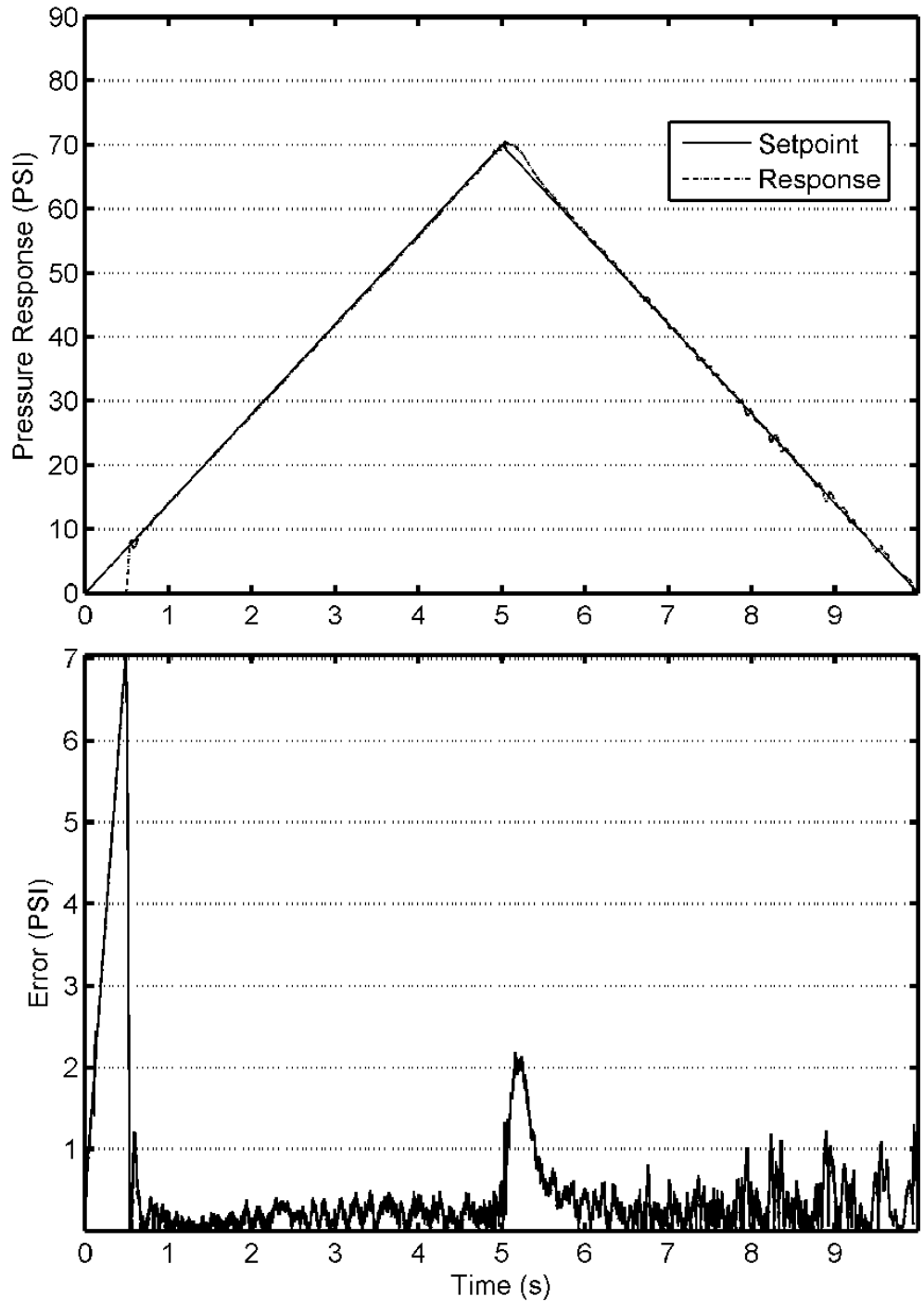
*B 2 Slow ramp response to PID*

**B.1 PID+ ENFF**

*B2.2 Fast Ramp*

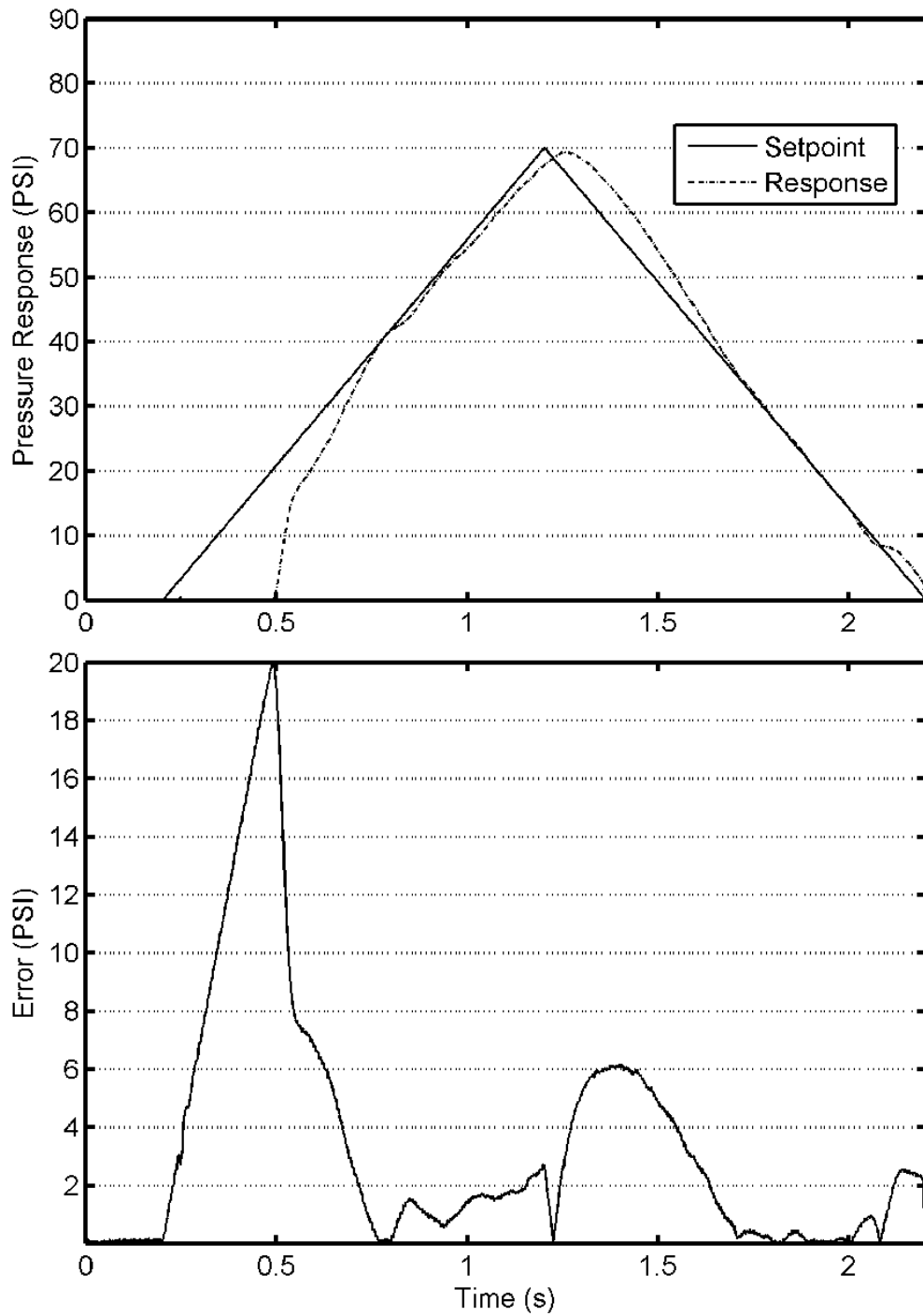


*B2.2 Slow ramp*

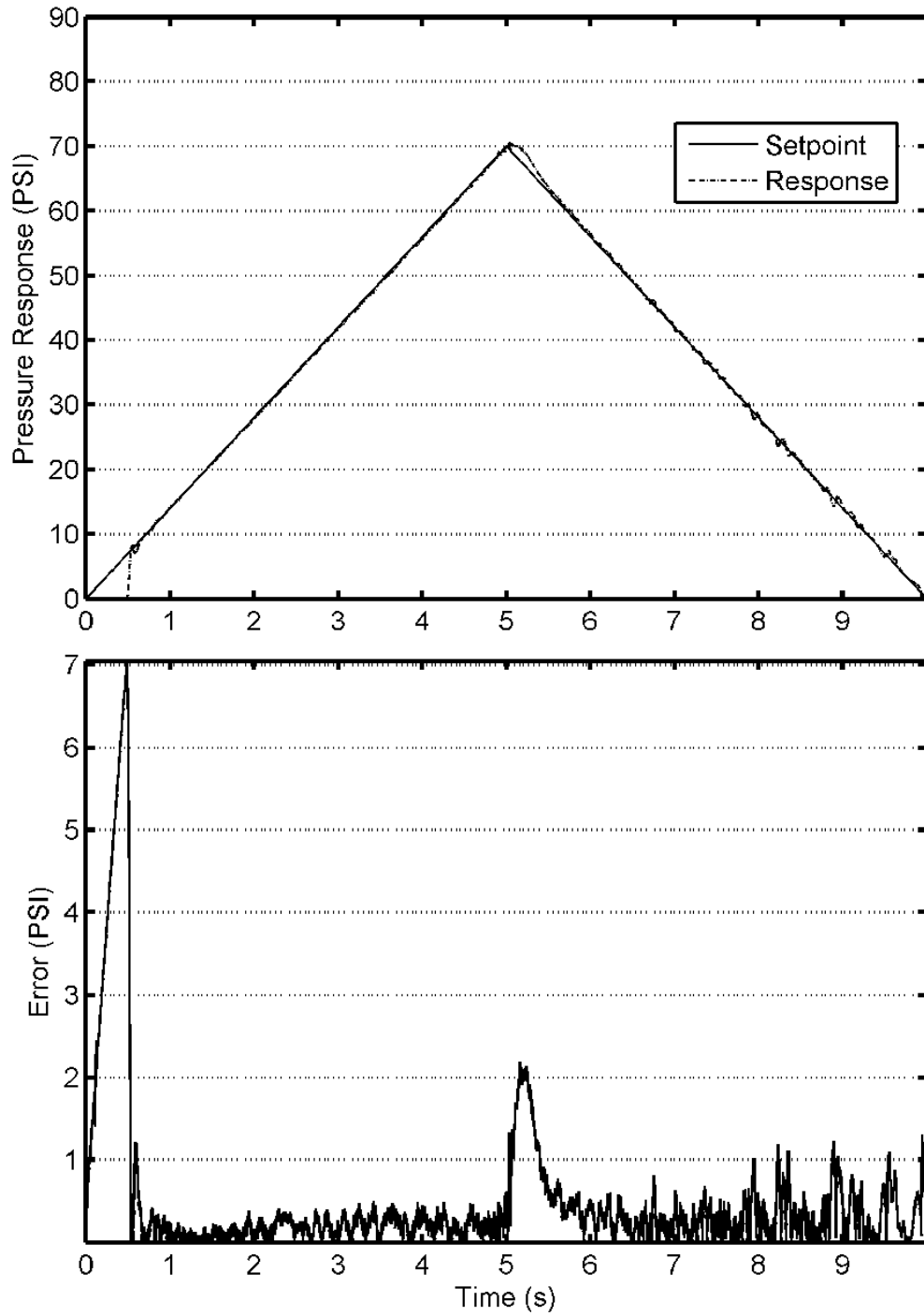


**EXTENDED PID**

***B3.1 Fast Ramp***

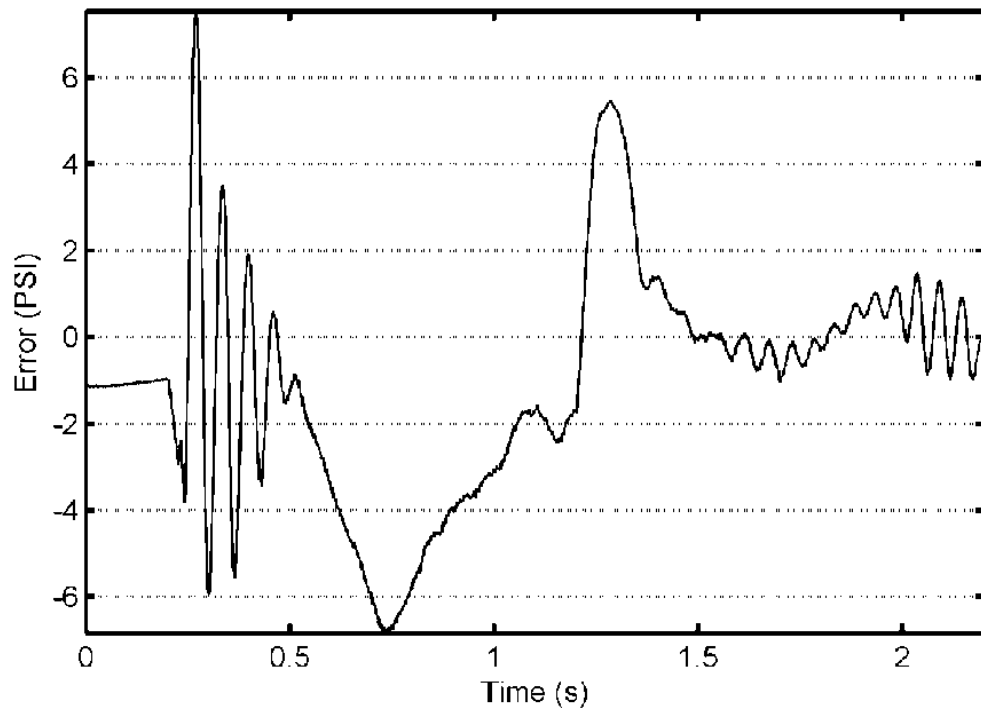
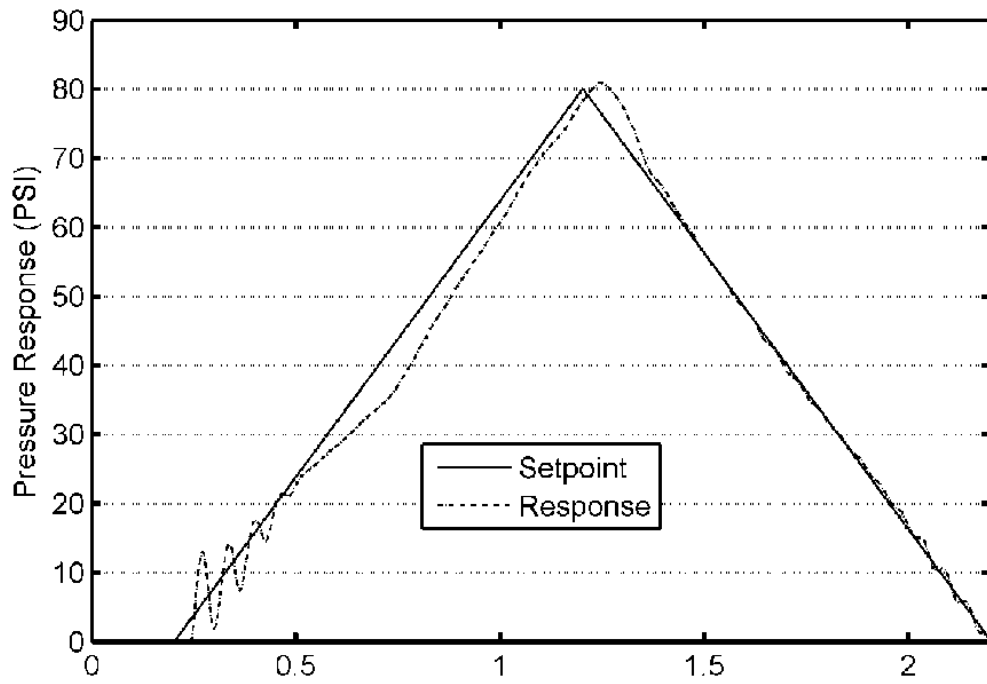


*B3.1 Slow ramp*

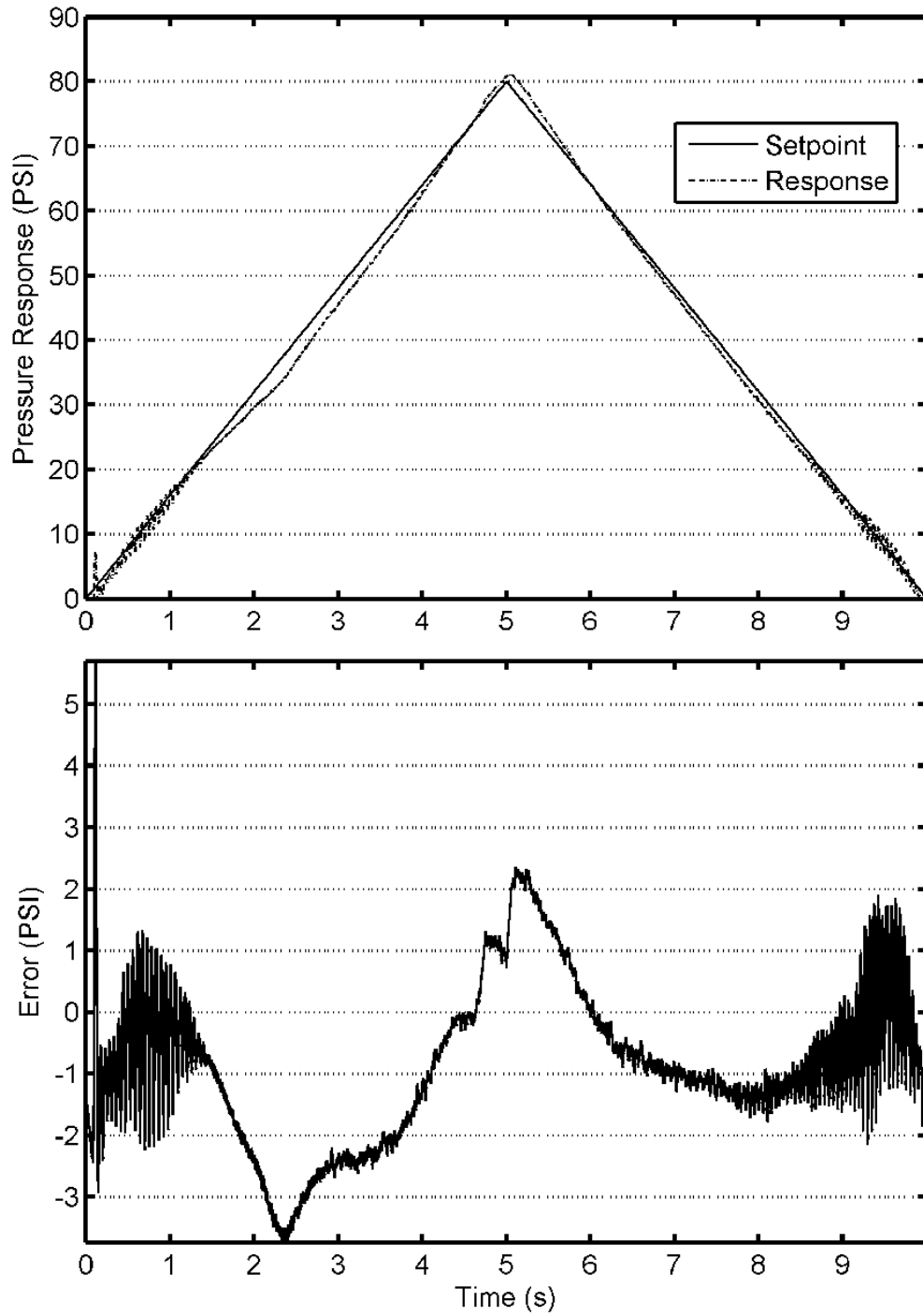


**ALTERNATIVE PID**

***B4.1 Fast ramp***



*Slow Ramp*



**APPENDIX C : TABULATED RESULTS****C1: PID***Table 7 PID Mean Error*

<b>Mean error results for PID controller (units are PSI)</b>							
<b>Setpoint</b>	<b>Test 1</b>	<b>Test 2</b>	<b>Test 3</b>	<b>Test 4</b>	<b>Test 5</b>	<b>Mean</b>	<b>Standard Deviation</b>
Step	1.771	1.764	1.767	1.772	1.738	1.763	0.012
Cosine	3.796	3.799	3.8145	3.852	3.807	3.814	0.019
Fast Ramp	2.153	2.173	2.198	2.186	2.211	2.184	0.018
Slow ramp	0.516	0.518	0.52	0.52	0.519	0.519	0.001

*Table 8 PID Mean Absolute*

<b>Mean abs. error results for PID controller (units are PSI)</b>							
<b>Setpoint</b>	<b>Test 1</b>	<b>Test 2</b>	<b>Test 3</b>	<b>Test 4</b>	<b>Test 5</b>	<b>Mean</b>	<b>Standard Deviation</b>
Step	7.444	7.320	7.231	7.339	7.194	7.306	0.080
Cosine	11.874	11.738	11.676	11.587	11.589	11.693	0.097
Fast Ramp	6.633	6.810	6.842	6.771	6.911	6.794	0.084
Slow ramp	1.705	1.651	1.640	1.715	1.641	1.671	0.030

*Table 9 Max Error*

<b>Max error results for PID controller (units are PSI)</b>							
<b>Setpoint</b>	<b>Test 1</b>	<b>Test 2</b>	<b>Test 3</b>	<b>Test 4</b>	<b>Test 5</b>	<b>Mean</b>	<b>Standard Deviation</b>
Step	78.917	78.898	78.965	78.927	79.013	78.944	0.037
Cosine	56.557	56.073	56.595	56.372	56.235	56.366	0.179
Fast Ramp	31.631	31.692	31.784	31.957	32.012	31.815	0.135
Slow ramp	13.729	13.697	13.733	13.739	13.735	13.727	0.014

**C2: PID+ENFF***Table 10 PIDENFF Mean error*

<b>Mean error results for PID+ENFF controller (units are PSI)</b>							
<b>Setpoint</b>	<b>Test 1</b>	<b>Test 2</b>	<b>Test 3</b>	<b>Test 4</b>	<b>Test 5</b>	<b>Mean</b>	<b>Standard Deviation</b>
Step	1.469	1.550	1.540	1.542	1.399	1.500	0.054
Cosine	3.448	3.500	3.525	3.601	3.353	3.485	0.075
Fast Ramp	1.352	1.435	1.444	1.447	1.402	1.416	0.033
Slow ramp	0.145	0.160	0.172	0.193	0.162	0.167	0.015

*Table 11 PIDENFF Mean ABS Error*

<b>Mean abs. error results for PID+ENFF controller (units are PSI)</b>							
<b>Setpoint</b>	<b>Test 1</b>	<b>Test 2</b>	<b>Test 3</b>	<b>Test 4</b>	<b>Test 5</b>	<b>Mean</b>	<b>Standard Deviation</b>
Step	5.352	5.265	5.366	5.360	5.300	5.329	0.036
Cosine	8.311	8.209	8.229	8.149	8.123	8.204	0.060
Fast Ramp	3.394	3.534	3.544	3.561	3.355	3.478	0.078
Slow ramp	0.546	0.598	0.636	0.641	0.606	0.605	0.031
Total	5.352	5.265	5.366	5.360	5.300	5.329	0.036

*Table 12 PIDENFF Max Error*

<b>Max error results for PID+ENFF controller (units are PSI)</b>							
<b>Setpoint</b>	<b>Test 1</b>	<b>Test 2</b>	<b>Test 3</b>	<b>Test 4</b>	<b>Test 5</b>	<b>Mean</b>	<b>Standard Deviation</b>
Step	70.410	70.343	70.372	70.382	70.343	70.370	0.023
Cosine	35.324	35.286	35.161	35.018	34.635	35.085	0.227
Fast Ramp	19.945	20.327	20.461	19.949	20.426	20.222	0.209
Slow ramp	7.178	7.091	7.080	7.214	7.239	7.160	0.059
Total	70.410	70.343	70.372	70.382	70.343	70.370	0.023

**C3 :EPID**

*Table 13 EPID Mean Error*

<b>Mean error results for EPID controller (units are PSI)</b>							
<b>Setpoint</b>	<b>Test 1</b>	<b>Test 2</b>	<b>Test 3</b>	<b>Test 4</b>	<b>Test 5</b>	<b>Mean</b>	<b>Standard Deviation</b>
Step	-0.569	-0.967	-0.558	-0.888	-0.598	-0.716	0.160
Cosine	-0.383	-0.463	-0.357	-0.478	-0.339	-0.404	0.052
Fast Ramp	-0.272	-0.163	-0.178	-0.247	-0.134	-0.199	0.048
Slow ramp	0.004	0.223	0.071	-0.110	0.099	0.058	0.100
Total	-0.569	-0.967	-0.558	-0.888	-0.598	-0.716	0.160

*Table 14 EPID Mean ABS Error*

<b>Mean abs. error results for EPID controller (units are PSI)</b>							
<b>Setpoint</b>	<b>Test 1</b>	<b>Test 2</b>	<b>Test 3</b>	<b>Test 4</b>	<b>Test 5</b>	<b>Mean</b>	<b>Standard Deviation</b>
Step	1.840	2.062	1.899	2.036	1.814	1.930	0.092
Cosine	1.361	1.445	1.292	1.371	1.285	1.351	0.054
Fast Ramp	0.849	0.884	0.799	0.840	0.795	0.834	0.030
Slow ramp	0.538	0.603	0.491	0.606	0.555	0.559	0.039

Table 15 EPID Max Error

<b>Max. abs. error results for EPID controller (units are PSI)</b>							
<b>Setpoint</b>	<b>Test 1</b>	<b>Test 2</b>	<b>Test 3</b>	<b>Test 4</b>	<b>Test 5</b>	<b>Mean</b>	<b>Standard Deviation</b>
Step	33.496	33.764	33.487	33.726	33.506	33.596	0.112
Cosine	3.423	3.347	3.307	3.198	3.109	3.277	0.101
Fast Ramp	2.346	2.415	2.007	2.277	2.250	2.259	0.126
Slow ramp	1.827	2.222	1.886	1.842	1.874	1.930	0.135

**C4 : APID**

APID Table 16 APID Mean Error

<b>Mean error results for APID controller (units are PSI)</b>							
<b>Setpoint</b>	<b>Test 1</b>	<b>Test 2</b>	<b>Test 3</b>	<b>Test 4</b>	<b>Test 5*</b>	<b>Mean</b>	<b>Standard Deviation</b>
Step	-1.908	-1.850	-1.798	-1.939	-2.489	-1.997	0.229
Cosine	0.379	0.863	1.277	1.006	0.557	0.816	0.291
Fast Ramp	0.708	1.090	1.357	1.290	0.815	1.052	0.233
Slow ramp	0.800	0.865	0.900	0.942	0.849	0.871	0.044

\*With test 5 the step test experienced a higher than normal level of oscillations.

Table 17 Mean ABS PID

<b>Mean Absolute error results for APID controller (units are PSI)</b>							
<b>Setpoint</b>	<b>Test 1</b>	<b>Test 2</b>	<b>Test 3</b>	<b>Test 4</b>	<b>Test 5*</b>	<b>Mean</b>	<b>Standard Deviation</b>
Step	6.264	6.541	6.627	6.711	7.061	6.641	0.236
Cosine	3.164	3.503	3.873	3.675	3.116	3.466	0.266
Fast Ramp	1.846	2.174	2.411	2.308	2.308	2.209	0.179
Slow ramp	1.337	1.512	1.596	1.594	1.606	1.529	0.093



*Table 18 EPID Max Error*

<b>Max. abs. error results for APID controller (units are PSI)</b>							
<b>Setpoint</b>	<b>Test 1</b>	<b>Test 2</b>	<b>Test 3</b>	<b>Test 4</b>	<b>Test 5</b>	<b>Mean</b>	<b>Standard Deviation</b>
Step	80.714	80.752	80.790	80.761	80.742	80.752	0.023
Cosine	9.654	14.536	17.486	16.496	10.475	13.729	2.876
Fast Ramp	6.254	7.514	8.631	7.807	6.592	7.360	0.780
Slow ramp	5.439	5.162	5.468	5.935	6.078	5.616	0.309
Total	80.714	80.752	80.790	80.761	80.742	80.752	0.023